DOI: 10.1002/anie.200603995

Microstructures

Multiphoton Fabrication

Christopher N. LaFratta, John T. Fourkas, Tommaso Baldacchini, and Richard A. Farrer*

Keywords:
lithography · microfabrication · nanostructures · nonlinear optics · polymerization

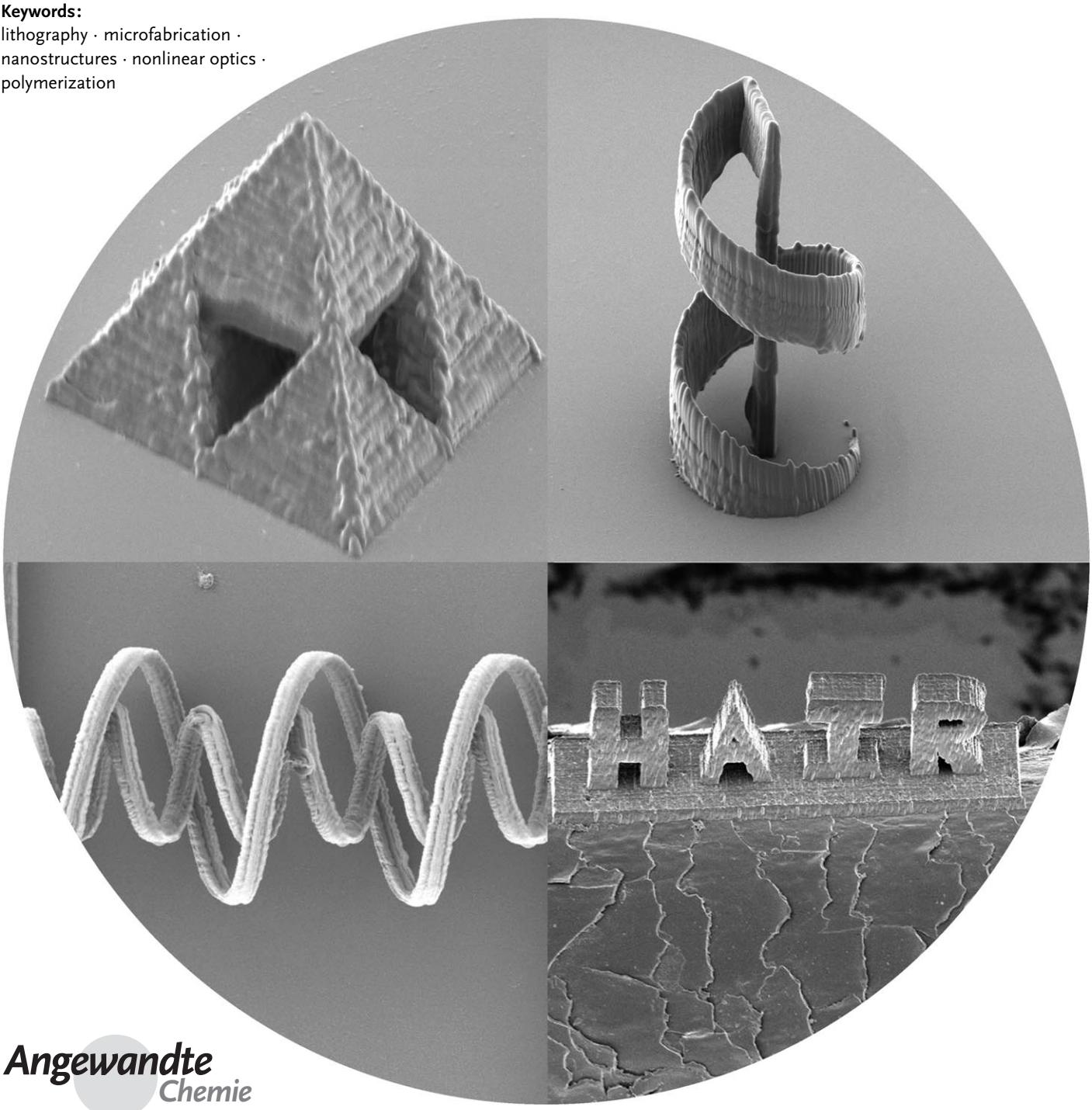

Chemical and physical processes driven by multiphoton absorption make possible the fabrication of complex, 3D structures with feature sizes as small as 100 nm. Since its inception less than a decade ago, the field of multiphoton fabrication has progressed rapidly, and multiphoton techniques are now being used to create functional microdevices. In this Review we discuss the techniques and materials used for multiphoton fabrication, the applications that have been demonstrated, as well as those being pursued. We also consider the outlook for this field, both in the laboratory and in industrial settings.

From the Contents

1. Introduction

Technological developments in microscopic pattern generation have driven the information revolution. The control processors of state-of-the-art computers will soon contain more than 1 billion transistors per square centimeter, with individual features on the scale of tens of nanometers. A comparable revolution is brewing for microtechnology of a different sort. What if all the benefits of speed, cost, and portability of microelectronics could be extended to mechanical, chemical, and medical systems? This is the basic concept behind emergent technologies such as microelectromechanical systems[1–4] (MEMS) and micro total analysis systems[5,6] (μTAS), which are poised to make major leaps in a broad range of applications in the near future.

Photolithography has been the dominant technique for microscale patterning for the past fifty years. By shrinking the size of electronic components and fabricating them in batches, huge leaps have been made in portability, speed, and cost. Recent improvements in the resolution of 193-nm immersion lithography have pushed feature sizes below a half pitch of 32 nm, which had been thought to be the limit of the technique.[7,8] This achievement is a technological marvel; however, a number of facets of conventional photolithography still pose constraints in its expansion into areas such as MEMS and μTAS. One problem is that the materials commonly used for photolithography require processing conditions that can be severe, including etching with harsh agents such as HF or reactive ions. Another issue is that photolithography is essentially a planar technique. By combining layers or using special release techniques, patterns can extend into the third dimension. However, the control currently available in the vertical dimension does not begin to approach what can be achieved in the other two dimensions.

To extend the range of materials that can be used in lithography, alternative patterning techniques have been developed, including dip-pen nanolithography,[9] nanoimprint lithography,[10] and soft lithography.[11,12] These techniques have some advantages over photolithography, such as higher resolution, more materials options, and gentler processing conditions. However, these techniques are also essentially two-dimensional.

Efforts to extend patterning capabilities into the third dimension have made the development of new techniques for 3D micro- and nanofabrication a highly active area of research. The most important approaches include ink-based writing,[13,14] self-assembly,[15] layer-by-layer assembly,[16,17] LIGA (lithography, electroplating, and molding),[18,19] and laser-based photolithographic techniques.

Writing with ink can be performed by either drop- or filament-based techniques, which are referred to as ink-jet printing[20,21] and robotic deposition,[22] respectively. A nozzle can deliver inks composed of colloids, polymers, or polyelectrolytes, whose rheological parameters can be tailored for the particular deposition technique. Structures can span a range of sizes, with the resolution of individual features ranging from roughly 1 to 100 μm. Although 3D control is possible in principle, in practice the inks are not rigid enough to create structures of arbitrary geometries. For example, ink-based writing of lattice-type scaffolds has been demonstrated, but, without the structural support of a lattice, freestanding individual lines cannot be created.

Self-assembly of 3D microstructures with arbitrary control of geometry is currently beyond reach in the laboratory, although its ultimate feasibility is clearly demonstrated by the countless examples provided in biological systems. Self-assembly techniques are currently best-suited for the creation

[*] C. N. LaFratta, Prof. J. T. Fourkas
Department of Chemistry and Biochemistry
University of Maryland
College Park, MD 20742 (USA)
Fax: (+1) 301-314-4121
E-mail: fourkas@umd.edu
Homepage: http://www.chem.umd.edu/faculty/fourkas
Dr. T. Baldacchini
Technology and Application Center
Newport Corporation
1791 Deere Avenue, Irvine, CA 92606 (USA)
Prof. R. A. Farrer
Chemistry Department
Colorado State University-Pueblo
2200 Bonaforte Blvd., Pueblo, CO 81001 (USA)

of periodic structures. For example, colloidal solutions can be dried carefully to yield close-packed colloidal crystals that can have optical properties similar to those of opals or inverse opals.[23] Block copolymers also self-assemble into useful periodic patterns in three dimensions.[24] DNA has also been used to great advantage in the self-assembly of 2D structures in recent years.[25] Research into self-assembly of nonperiodic, 3D microstructures is still in its infancy.

Layer-by-layer assembly creates 3D structures by stacking planar patterns, which can be made by using the 2D patterning techniques discussed above. A variety of materials can be used for layer-by-layer assembly. However, the 3D structures that are produced have geometric limitations that arise from mechanical constraints. For example, in many layer-by-layer techniques, each point fabricated in a layer must be attached either to another point in the layer or to a point in the layer below. This means that some features, such as the downward serif at the top right of the letter "Γ", cannot be fabricated in a layer-by-layer approach. Layer-by-layer techniques also require a large number of processing steps and suffer from problems of registration.[26]

Another process that can extend fabrication into the third dimension was developed in the early 1980s and is now known as LIGA.[27,28] LIGA is a German acronym for X-ray lithography (Lithographie), electroplating (Galvanoformung), and molding (Abformung). In this method, X-rays are used to create patterns. Synchrotron-generated X-rays have small divergence angles owing to their extremely short wavelength, which allows patterning in photoresists with micrometer resolution and depths that can exceed 1 cm. The result is high-aspect-ratio patterns, such as channels and gears, that can be used as molds to electrodeposit metals, such as nickel. The metal pattern can be used as is, or its shape can be inverted again by using the metal pattern as a mold for polymer parts. Structures made by LIGA have smooth surfaces and sharp vertical features, but are of limited 3D complexity because of the line-of-sight nature of the X-ray exposure.

Laser-based techniques such as holographic lithography and phase-mask lithography have also been developed to create periodic 3D patterns. In holographic lithography, which is also known as multibeam interference lithography (MBIL), two or more nonparallel laser beams are incident on a photoresist.[29–31] The resulting light intensity distribution is captured within the photoresist, resulting in periodic voids based on the interference pattern of the light. Phase-mask lithography also relies on interference to generate a periodic pattern within a photoresist but, instead of using multiple beams, a single beam is transmitted through a phase mask, which creates a complex 3D distribution of light to expose the photoresist.[32] Both of these techniques are promising methods for the rapid preparation of 3D patterns; however, they are inherently restricted to locally periodic patterns because they take advantage of the periodic nature of light to define the features and therefore are not capable of arbitrary patterning in three dimensions.

Unlike the previous techniques described, fabrication by a focused laser can allow for true 3D control. Laser chemical

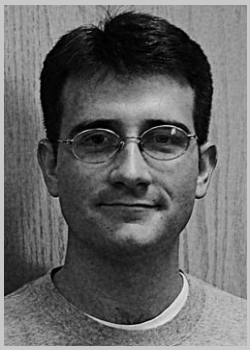

Christopher LaFratta was born in Malden, Massachusetts, USA, in 1979. He received a BS in chemistry from the University of Massachusetts, Dartmouth, in 2001. He then joined the laboratory of Prof. John Fourkas at Boston College, where his research focused on aspects of multiphoton fabrication. After the research group moved to the University of Maryland, College Park, he received his PhD in 2006. He was then awarded an NIH TEACHRS postdoctoral fellowship to work in the group of Prof. David Walt at Tufts University on the development of a microarray-based universal chemical sensing platform.

Tommaso Baldacchini was born in Rome, Italy, in 1973. After studying chemistry at the University of Rome "La Sapienza", he pursued doctoral research at Boston College, where he worked on unconventional methods to fabricate 3D microstructures. He received a PhD in chemistry in 2004. As a postdoctoral researcher with Prof. Eric Mazur at Harvard University he investigated the wettability properties of nanostructured surfaces prepared by laser ablation. In 2006 he joined the Technology and Application Center at Newport Corporation as a Senior Scientist. His research interests lie in applications of nonlinear optics in microscopy and nanofabrication.

John T. Fourkas received a BS and an MS in chemistry from the Caltech in 1986, and a PhD in chemistry from Stanford University in 1991. He worked at the University of Texas at Austin and MIT as an NSF Postdoctoral Fellow. He joined the chemistry faculty at Boston College in 1994, and then moved to the University of Maryland, College Park, in 2005, where he holds the Millard Alexander Chair in Chemistry. He is a Fellow of the American Association for the Advancement of Science, the American Physical Society, and the Optical Society of America. His research interests include applications of nonlinear optics in spectroscopy, microscopy, and fabrication.

Richard A. Farrer was born in 1968 in Grand Rapids, MI. He received his BSc degree from Aquinas College (Michigan) in 1991. He attended graduate school at Boston College and received his PhD in chemistry with Prof. John T. Fourkas in 2001. He remained at Boston College as a postdoctoral researcher with Prof. Fourkas until 2005. He is currently an assistant professor in the Chemistry Department at Colorado State University in Pueblo with research interests that include the development of three-dimensional microscopic devices and the production and properties of nanoparticles.

machining, for example, is capable of etching or depositing material in a liquid or gaseous environment.[33,34] Microstereolithography uses a laser to harden the surface of a prepolymer resin into 2D pattern.[35–39] Additional resin is then flowed onto the pattern to create a new surface, and the process is repeated until the part is finished. Any unhardened resin is washed away with solvent. 3D parts of considerable complexity can be created with this technique, although the fabrication is slow and high precision is required in the resin reflow step.

Multiphoton absorption (MPA) offers another means of fabricating 3D structures. Because MPA depends nonlinearly upon intensity, it is possible to localize photochemical or photophysical material transformations within the focal volume of a laser beam that has passed through a microscope objective. Complex structures can be fabricated by moving the laser focus in three dimensions relative to the substrate. Multiphoton techniques offer true 3D fabrication capability at resolutions lower than 100 nm with a straightforward experimental setup.

In this Review we summarize the principles of MPA-based fabrication. We discuss the fundamental principles of MPA, the types of materials that have been patterned, as well as applications and future prospects for the technology.

2. Multiphoton Absorption

The process of MPA was first predicted theoretically in 1931 by Maria Göppert-Mayer.[40] Because of the high photon intensities required, even two-photon absorption (TPA) was not demonstrated until the advent of the laser.[41] The basic requirement for MPA is that an absorption event is caused by the collective action of two or more photons, all of which must be present simultaneously to impart enough energy to drive a transition. For example, in TPA the sum of the two photon energies is resonant with the energy of the transition that is driven. The most common implementation of TPA in fabrication is for both photons to have the same energy, but this need not be the case.

There is a strong analogy between MPA of n photons and the rate of a concerted chemical reaction involving n molecules. For the reaction $n\,\mathrm{A} \rightarrow \mathrm{A}_n$ to occur concertedly, n molecules of A must be in the same place at the same time. As a result, the rate of the reaction is proportional to $[\mathrm{A}]^n$. By the same token, the rate of MPA for n photons is proportional to the concentration of photons (i.e., the intensity) to the nth power.

It is common to employ ultrafast lasers to drive MPA. A typical ultrafast Ti:sapphire laser produces pulses that are a few tens of femtoseconds in duration at a repetition rate of approximately 80 MHz, which corresponds to an interpulse separation of about 12 ns. The instantaneous intensity during a pulse is quite high, which is favorable for MPA. However, because the pulses are five to six orders of magnitude shorter than the repetition period of the laser, the average power is low.

The nonlinear intensity dependence of the absorption process allows the excitation to be localized within the focal volume of a laser beam. To see how this process works, consider a sample in which the absorbing molecules are distributed homogeneously. The rate of absorption in a transverse cross section of a laser beam depends upon the product of the intensity (number of photons per time per area) and the number of molecules in the cross section (which is proportional to the area). Thus, the absorption rate does not depend upon area. The number of molecules excited by single-photon absorption is constant in any transverse plane of a focused laser beam, and so there is no localization of excitation in the focal region (Figure 1, left).

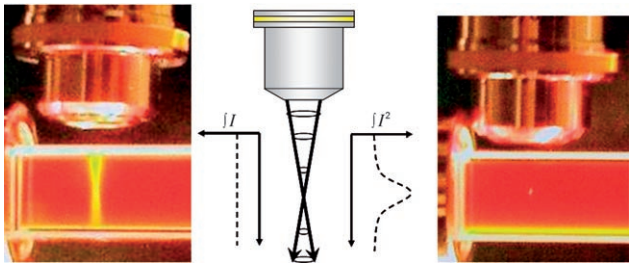

Figure 1. Fluorescence from a solution of rhodamine B caused by single-photon excitation from a UV lamp (left) and by two-photon excitation from a mode-locked Ti:sapphire laser operating at a wavelength of 800 nm (right). The integrated intensity in each transverse section of the beam does not depend upon position for single-photon excitation, but is tightly peaked in the focal region for two-photon excitation.

In the case of TPA, the rate of absorption in a transverse cross section of a laser beam is proportional to the intensity squared times the number of molecules in the cross section. The absorption rate therefore scales inversely with area. The greatest density of excited molecules will therefore be in the region in which the laser beam is focused most tightly (Figure 1, right). This localization was first utilized in 1990 by Denk, Strickler, and Webb in two-photon fluorescence microscopy (TPFM).[42] In TPFM, the excitation wavelength used is usually approximately double the peak absorption wavelength of a given fluorophore. TPA occurs at the focal point, inducing fluorescence that can be imaged. Since this seminal work, hundreds of groups around the world have used MPA for fluorescence imaging techniques,[43,44] 3D data storage,[45] photodynamic therapy,[46] and microfabrication.[47–52]

In almost all of these applications of MPA, objectives with high numerical aperture (NA) are employed to create the photon density needed for nonlinear absorption. For an ultrafast laser with a pulse duration τ and a pulse repetition rate f_p, the number of photons absorbed per molecule per pulse is given by Equation (1),[42] in which p_0 is the time-averaged laser power, λ is the excitation wavelength, and δ is the two-photon absorption cross section.

$$n_a \approx \frac{p_0^2 \delta}{\tau f_p^2} \left(\frac{(\mathrm{NA})^2}{2\hbar c \lambda} \right)^2 \qquad (1)$$

The units for δ are named Göppert-Mayer (GM), after the Nobel-laureate physicist, and are defined in SI units as

$1\ \mathrm{GM} = 10^{-58}\ \mathrm{m^4\,s\,photon^{-1}}$. As an example, δ for fluorescein, a good two-photon-absorbing fluorophore, is 38 GM.

Figure 2 shows a typical experimental setup for multiphoton fabrication. The excitation source is a mode-locked Ti:sapphire laser, which typically produces pulses with a

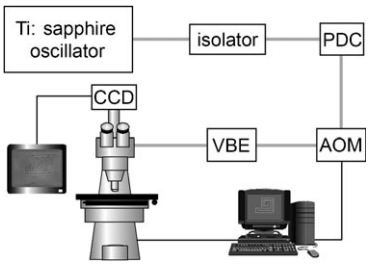

Figure 2. Schematic of a typical experimental setup for multiphoton fabrication. PDC = prism dispersion compensator, AOM = acoustooptic modulator, VBE = variable beam expander, CCD = charge-coupled device camera.

duration of tens to hundreds of femtoseconds and a center wavelength of 800 nm. The repetition rates for these lasers is on the order of 80 MHz, and the average output power can range from hundreds of milliwatts to more than a watt. An isolator, such as a Faraday rotator, is often placed in the beam path to prevent interference from reflected light. Dispersion of the laser pulses can be compensated for by a pair of prisms to obtain the shortest possible pulses at the sample. The intensity of the laser can also be controlled by a device such as an acoustooptic modulator, an electrooptic modulator, or a shutter. The beam is generally expanded so as to overfill the back aperture of the objective, although a variable beam expander can be used if one wishes to control the degree of focusing to manipulate the dimensions of the region in which fabrication occurs.

Although a mounted objective is sufficient for fabrication purposes, using a microscope is convenient for sample positioning and viewing and for being able to switch objectives rapidly. In the experimental setup shown in Figure 2, the laser beam enters through the reflected-light port of an upright microscope and is directed into the objective by a beam splitter. The sample rests on a computer-controlled stage that can be translated in three dimensions relative to the focus of the laser beam; an alternative approach is to employ scanning mirrors to move the focal point relative to the sample. Transmitted light is used to view the sample with a CCD camera and a video screen, simplifying the positioning of the sample and making it possible to monitor fabrication in real time.

3. Multiphoton Absorption Polymerization

The most well developed of multiphoton fabrication techniques is multiphoton absorption polymerization (MAP). In this method, the sample is a prepolymer resin containing a photoinitiator that can that can be excited by MPA. The resins most commonly used act as negative-tone photoresists, that is, polymerization occurs in the regions that are exposed. However, MAP prepolymer resins that act as positive-tone photoresists, that is, ones in which the unexposed regions are hardened, have also been demonstrated. After exposure, a development process is used to remove any unhardened material. Development generally involves washing with one or more solvents, and can also involve additional processing steps such as baking.

In this section we examine the photoinitiators and polymers that have been used in MAP fabrication and discuss the physical properties of the structures produced.

3.1. MAP Materials

3.1.1. The Prepolymer Resin

To prevent components from moving during fabrication, the prepolymer resin used for MAP is usually a viscous liquid, an amorphous solid, or a gel. Each of these options has its own advantages and disadvantages. Liquid samples are simple to prepare and process, but can allow undesired motion of structures during fabrication. Solids and gels are more difficult and time-consuming to prepare and process, but the complete restriction of motion in these media facilitates the fabrication of complex structures, such as those with free-moving parts.

There are two crucial components in a prepolymer resin for MAP: the photoinitiator and the monomers. Other components can include polymerization inhibitors (to stabilize the resin and influence the feature size), solvents (to assist in casting), filler polymers (to create gels or increase the viscosity of liquid resins), and other additives (such as dye molecules) that introduce new function to polymerized structures. In the following subsections we discuss the types of polymer systems that have found the greatest use in MAP.

3.1.2. Radical Polymerization

The majority of the MAP research reported to date has involved radical polymerization. The popularity of radical polymerization in MAP stems from a combination of high reaction rates, ease of processing, and wide availability of photoinitiators and monomers for this type of chemistry.

3.1.2.1. Radical Photoinitiators

The first step in radical polymerization is the nonlinear excitation of a photoinitiator, which can either cleave homolytically or transfer its energy to a coinitiator to create the radicals that begin the polymerization reaction. Photoinitiators that operate by these mechanisms are classified as type I and type II, respectively, although type I initiators can also be used as type II initiators. One requirement for either type of photoinitiator, if it to be useful in MAP, is that it not absorb light in the near-infrared and in the red portion of the spectrum.

The utility of a radical photoinitiator for MAP depends upon a balance among a number of different parameters. Efficient polymerization is promoted by a high value of δ, a

high radical yield (Φ_r), and a high initiation velocity. However, solubility is also an important consideration. A highly soluble photoinitiator of modest efficiency may be preferable to a sparingly soluble initiator of high efficiency, for example.

We first consider Norrish type I radical initiators. Several groups have synthesized custom type I photoinitiators that are optimized for TPA, making fabrication possible at low laser powers. Similar molecules engineered in this manner can be used for other applications that take advantage of TPA, such as optical data storage, optical limiting, photodynamic therapy, and two-photon imaging. Work in this field centers on molecules composed of a conjugated central region flanked by electron-donating (D) or -accepting (A) groups. The various core moieties that have been used for MAP initiators include (*E*)-stilbene, bis(stryl)benzene, naphthalene, biphenyl, and fluorene.

Marder, Perry, and co-workers have done extensive work on the (*E*)-stilbene and bis(stryl)benzene systems, symmetrically altering the strength and positions of electron-donating and -accepting groups.[53–56] Configurations such as D-π-D, D-π-A-π-D, and A-π-D-π-A (π represents a conjugated bridge) have been tested, and molecules with δ values as high as 1250 GM have been synthesized.[53] Studies show that symmetric charge transfer from the molecular center to the ends (or vice versa) is responsible for high δ values. Extending the conjugation length increases the value of δ, as does increasing the electron-donating or -accepting strength. A side effect of these changes is a shift of the TPA maximum to longer wavelengths with increasing conjugation length. This shift allows molecules to be optimized for different wavelengths, but for the most common case of 800-nm excitation, shifted TPA spectra also lead to inefficient pumping. After this type of molecule has been excited by TPA it is thought to undergo direct electron transfer to an acrylate monomer/oligomer, initiating the polymerization reaction. Thanks to its high δ value, 4,4′bis(*N*,*N*-di-*n*-butylamino)-(*E*)-stilbene has been used for MAP at powers as low as a few hundred microwatts with a Ti:sapphire oscillator.[54] Since the polymerization efficiency is proportional to the product of δ and Φ_r, the high TPA cross sections of these molecules evidently more than compensate for low radical yields.

Building on the work of Marder, Perry, and co-workers, Watanabe and co-workers showed that a custom photoinitiator with a cyano-substituted imino core could effectively initiate MAP with a tightly focused Ti:sapphire oscillator.[57] They also confirmed, by comparing different photoinitiators, that a high δ value alone is not sufficient for rapid polymerization.

Prasad, Reinhardt, and co-workers developed the initiator 6-benzothiazol-2-yl-2-naphthyl diphenylamine (AF183) and incorporated it into a mixture of commercial resins NOA 72 (Norland Products) and EPO-TEK 301 (Epoxy Technology) for use in MAP.[58] AF183, an unsymmetric molecule with a δ value of 6840 GM, is part of series of molecules optimized for strong TPA at 800 nm.

The biphenyl and fluorene systems have also been studied by Prasad, Reinhardt, and co-workers[59–62] and have been applied to MAP by Belfield, Van Stryland, and co-workers.[63] Like the (*E*)-stilbene and naphthalene systems, these conjugated units provide a bridge for charge transfer. It has been found that locking the planarity of the biphenyl system by bridging it into a fluorene system can enhance this charge transfer. The initiator used by Belfield and co-workers was a diphenylaminobenzothiazolylfluorene analogue of the form D-π-A. This asymmetric motif takes advantage of the fact that polar molecules have a large change in dipole moment during excitation through a virtual state and therefore have a correspondingly high value of δ. This initiator was used to polymerize acrylic monomers by using an amplified Ti:sapphire system with an average power of a few milliwatts and a repetition rate of 1 kHz.[63]

Andraud and co-workers have also used a substituted fluorenyl system to initiate MAP.[47] They used this initiator to demonstrate fabrication with an inexpensive, frequency-doubled Nd:YAG microlaser that produces 0.5-ns pulses at 532 nm with a repetition rate of 6.5 kHz.[64,65] The aminobiphenyl-substituted fluorene is of the D-π-D type and has a δ value of 80 GM at 532 nm. Acrylic monomers have been polymerized with an average power of around 1 mW. This group has also reported TPA of 1064-nm light in symmetric photoinitiator molecules composed of a central ketone electron-accepting group attached to two electron-donating groups by conjugated bridges. The δ value for such molecules is about 100 GM at 1064 nm, and the intensity threshold for fabrication is roughly twice that for initiation at 532 nm.

There are many commercially available examples of type I initiators, most of which are aromatic carbonyl compounds. Electronic excitation of these molecules generally leads to the creation of a singlet $\cdot$C-O$\cdot$ diradical that undergoes intersystem crossing to a triplet diradical state with a lifetime on the order of 100 ps and subsequent rapid homolytic α-cleavage.[66]

SCR500 (Japan Synthetic Rubber Co.) is a popular MAP resin composed of urethane acrylate oligomers (molecular weights 480 and 1200) and two type I photoinitiators (Irgacure 369 and Irgacure 184).[48] This resin has been polymerized with just a few milliwatts of average power from a Ti:sapphire oscillator through a high-NA objective. Irgacure 369 and 184 both have two-photon cross sections of approximately 20 GM, which is a typical value for the commercial compounds that have been measured.[67]

Another commercial acrylic resin that has been used for MAP is Nopcocure 800 (Japan Synthetic Rubber Co.).[68–71] Frequency-doubled light from a regeneratively amplified Ti:sapphire laser operating near 800 nm was used to make gears[70] and photonic crystal structures[68,69] using this resin.

An alternative to using a premixed commercial resin is to use a commercially available photoinitiator combined with selected monomers or oligomers to create a tailored resin with specific properties. Photoinitiators such as Irgacure 819 (bis(2,4,6-trimethylbenzoyl)phenylphosphine oxide), BME (2-methoxy-1,2-diphenylethanone), and ITX (2-/4-isopropylthioxanthone) have been used for MAP with custom acrylate or methacrylate resins.[63,72]

Our group has worked extensively with a commercially available acylphosphine oxide photoinitiator known as Lucirin TPO-L.[73–76] The UV/Vis absorption of Lucirin TPO-L arises from an n→π* transition. Upon excitation

and intersystem crossing the molecule photocleaves to form carbonyl and phosphinoyl radicals, resulting in the efficient initiation of the polymerization chain reaction. Although the TPA cross section of Lucirin TPO-L is small,[77] MAP with this photoinitiator generally requires only a few milliwatts of average power from a Ti:sapphire oscillator. The high efficiency of Lucirin TPO-L as a photoinitiator results from a combination of its high radical yield, highly reactive radical products, and high solubility. Another advantage of Lucirin TPO-L is that it is a liquid at room temperature and so can be mixed quickly, and at high weight percentages, with high-viscosity monomer or oligomer components. Thus, samples can be prepared in a few minutes or hours; in contrast, dissolving solid photoinitiators is a slow process that can take as long as days or even weeks.

Several groups have also demonstrated type II radical polymerization by using custom resins. Type II photoinitiators are used with a coinitiator, which is generally a bulky tertiary amine. This reaction takes place when the excited photoinitiator forms an exciplex and abstracts an α-hydrogen atom from the amine, which is followed by electron transfer.

Campagnola, Pitts, and co-workers have used several xanthene-based chromophores, including Rose Bengal, erythrosin, and eosin, in combination with the coinitiator triethanolamine, for the radical polymerization of acrylates, acrylamides, and biopolymers.[78,79] These chromophores all have δ values of about 10 GM at 800 nm, and approximately 100 mW of the output of a Ti:sapphire oscillator was required with a 0.75-NA objective to create structures. Campagnola and co-workers also performed MAP using 9-fluorenone-2-carboxylic acid with triethanolamine at an excitation wavelength of 780 nm, which is approximately three times its maximum single-photon absorption wavelength (260 nm).[79] This is the first clear demonstration of three-photon polymerization.

Belfield and co-workers used the commercial fluorone dye H-NU 470, along with the aryl amine *N*,*N*-dimethyl-2,6-diisopropylaniline (DIDMA), for type II radical polymerization of acrylates and methacrylates.[63] Single-photon absorption studies suggest the mechanism of initiation involves electron transfer from the aryl amine to the excited H-NU 470 followed by proton transfer from the aryl amine radical cation to H-NU 470; the resulting radical aryl amine initiates the polymerization reaction. ITX has also been used as a type II initiator in combination with DIDMA.[63] Both this system and H-NU 470 have been used for MAP with an amplified Ti:sapphire laser.

Li et al. reported the use of 7-diethylamino-3-(2′-benzimidazolyl)coumarin with a coinitiator of diphenyliodonium hexafluorophosphate.[80] They were able to achieve fabrication at average powers of less than 1 mW with a Ti:sapphire oscillator tuned to 800 nm. Watanabe and co-workers have used this iodonium coinitiator with their cyano-substituted, imino-backbone chromophore and a tertiary amine to enable fabrication with acrylates in dioxane.[81]

The photoinitiators that have been used for radical MAP vary from small molecules to large conjugated molecules to ternary systems. Many groups have designed custom photoinitiators that require low threshold powers and allow less expensive laser systems to be employed. Although the benefits of custom initiators are clear, their availability is limited. Commercial resins or resins that employ commercial photoinitiators have the benefit of accessibility but generally have slightly higher power thresholds for fabrication. However, the fabrication threshold for all of the systems discussed herein is well below the available power of the lasers used, and therefore the use of commercial photoinitiators is entirely practical.

3.1.2.2. Materials for Radical Polymerization

The majority of the resins used in the studies described above employed acrylate monomers. Acrylic resins have a number of properties that make them attractive for MAP. Acrylates are used extensively in industry and so are commercially available in a wide assortment of functionalities, sizes, and compositions. They are easily processed by spin coating or drop casting. The nonpolymerized resins are soluble in common solvents such as ethanol. Polyfunctional acrylates result in polymeric solids that are highly cross-linked and are therefore able to resist swelling during the development step after fabrication. Acrylic structures are also inert enough to withstand many harsh solvents as well as elevated temperatures. Acrylic microstructures exhibit low shrinkage and have favorable mechanical properties. The polymerized solids are transparent in the visible region and are of high optical quality. Perhaps the most important quality of acrylates, however, is the high speed at which they polymerize. Rapid polymerization enables the use of fast scanning speeds, which is of fundamental importance in a serial process such as MAP.

Electron micrographs of typical structures created from acrylic resins are shown in Figure 3a–c. The interpenetrating microcoils in Figure 3a demonstrate the complexity of the structures that can be created with MAP. Figure 3b shows a cantilever with a high aspect ratio, a structure that could be created only with great difficulty by using conventional microstereolithography. The microbull in Figure 3c is perhaps the most famous structure created with MAP.[82] The degree of detail on this structure underscores the high resolution of this technique.

Acrylic resins are usually used in a pure liquid form, and a sample can be prepared by simply putting a drop onto a cover glass. Binders can also be combined with the acrylate monomers to form a gel. As an example, equal parts of the alkoxylated trifunctional acrylates (SR9008) and tris(2-hydroxyethyl)isocyanurate triacrylate (SR368) can be mixed with approximately 1% w/w photoinitiator and then combined with a poly(styrene-*co*-acrylonitrile) polymer binder in a 3:1 ratio.[54,57,64,83] The binder is dissolved in dioxane and mixed with the monomers, after which the sample is cast. After the solvent evaporates, the resulting film is rigid, allowing structures such as links on a chain to be made without fear of the resin reflowing (Figure 3d). Reflowing otherwise occurs easily if the resin is sandwiched between a coverslip and a slide with an oil-immersion objective pressing on it. Although the binder allows the creation of a sample that

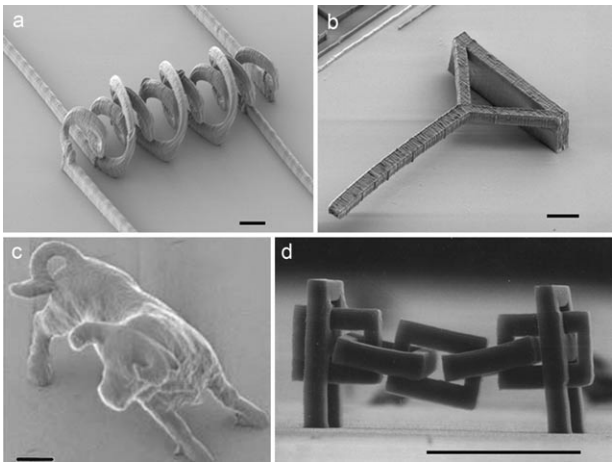

Figure 3. Scanning electron micrographs of structures created by MAP: a) interpenetrating microcoils, b) a cantilever, c) a microbull (reproduced from reference [82]), and d) a chain with interlocking rings (reproduced from reference [83]). The scale bars are 10 μm in (a) and (b), 2 μm in (c), and 100 μm in (d).

cannot flow, its preparation is time-consuming because solvent evaporation may take days.

Hydrogel materials made of acryloylacetone, acrylamide, and *N*,*N*′-bisacrylamide have also been fabricated by MAP.[84] These materials undergo a tautomerization after exposure to UV light, resulting in controllable shrinkage of the structures. Watanabe et al. produced a cantilever by using this material with an irreversible photoactuated process.[84]

Organically modified ceramics (ORMOCERs or ceramers) have also been used in MAP.[85] These silicate-based materials combine the best features of sol–gel processing and organic polymers.[86] They have an inorganic (-Si-O-Si-) backbone functionalized with organic groups such as acyrlates or epoxides. The organic side chains can cross-link the resin into a durable, biocompatible solid. In fact, such compounds are often used as photocurable dental composites.

Another material that has been used in MAP is polydimethylsiloxane (PDMS). This material is ubiquitous in soft lithography, where it is used for making 2D patterns with nanometer resolution.[12] Ober and co-workers reported photopolymerization of PDMS by two distinct methods.[87] The first was a photohydrosilylation reaction using a photoactive platinum catalyst. This method suffers from undesired thermal polymerization, which adversely affects the resolution that can be attained. The second method employed ITX to initiate cross-linking of the dimethylvinyl-terminated siloxane components, and did not exhibit any thermal polymerization.

3.1.3. Cationic Polymerization

An alternative mechanism to radical polymerization is cationic polymerization. A cationic photoinitiator works by generating a strong Brønsted acid that is capable of polymerizing epoxides and vinyl ethers. This photoacid is catalytic, and so each photoacid generator (PAG) molecule can initiate multiple polymerizations. Although singlet oxygen can quench radical polymerization, it does not affect cationic polymerization.

3.1.3.1. Cationic Photoinitiators

Diaryl iodonium and triaryl sulfonium salts are two classes of commercial PAG molecules that have been used in MAP. Both can be used alone or with a photosensitizer. Belfield et al.[63] used these salts alone to polymerize a diepoxide resin (Sartomer K-126).[63] Boiko et al. added ITX to diaryl iodonium hexafluoroantimonate and reported threshold polymerization intensities of around 1 $GW\,cm^{-2}$ with a Ti:sapphire oscillator.[63,88]

Two groups have reported the use of custom-made PAGs. Ober and co-workers[89] used the coumarin iodonium salt first reported by Li et al.[80] because of its high TPA cross section. Marder, Perry, and co-workers adapted their high-δ molecules with the bis(styryl)benzene core into PAGs by changing the pendant groups to contain sulfonium moieties.[90] The resulting molecule, labeled BSB-S_2, has a δ value of 690 GM and is more than ten times as sensitive as commercial cationic photoinitiators.

3.1.3.2. Materials for Cationic Polymerization

Epon SU-8, the most widely used epoxy polymerized by MAP,[91–93] has eight epoxy groups per monomer and contains a triaryl sulfonium salt PAG. SU-8 is used extensively in the conventional photolithography of MEMS because of its ability to be cast in films up to 500 μm thick that can yield structures with high aspect ratios. The availability and well-documented use of SU-8 make it a convenient choice as a cationic resin. For example, Teh et al.[92] have performed an extensive study of MAP with SU-8. Using a low-NA objective it was shown that structures with high aspect ratios (50:1) could be made with pulse energies of about 1.0 nJ. Generally, SU-8 requires additional processing steps, such as a pre- and postexposure baking; however, Misawa and co-workers showed recently that the postexposure baking can be eliminated because of the heating during exposure. The resulting features are approximately twice as small as those that underwent a postexposure treatment.[94]

Another commercial epoxy resin that has been used is SCR-701 (Japanese Rubber Co.). Originally designed for microstereolithography, SCR-701 has been used to make microgears and nanotweezers by Maruo et al.[95]

The PAGs used for cationic polymerization can also be used in positive-tone photoresists, which promises to be a useful way to fabricate 3D microfluidic devices. Marder, Perry, and co-workers demonstrated positive-tone MAP with the initiator BSB-S_2 in a random copolymer consisting of tetrahydropyranyl methacrylate, methylmethacrylate, and methacrylic acid units.[96,97] The tetrahydropyranyl ester groups are converted into carboxylic acids after the photoacid protolysis, causing them to be soluble in a basic developer. Channels 4 μm × 4 μm in cross section have been made 10 μm below a surface by using an average power of 40 μW from a Ti:sapphire oscillator.

3.2. Physical Properties of Structures Fabricated with MAP

3.2.1. Resolution

One important aspect in many applications of MAP is the size and shape of the volume elements (voxels). The accurate measurement of voxel dimensions is a considerable challenge. An issue that must always be considered is the truncation effect. For a structure (or an individual voxel) to remain after washing, it must be in contact with the substrate. Such contact requires that the focal point of the beam be partially submerged in the substrate. Under such conditions only a partial voxel is created. If more than half of the focal volume is below the substrate, the observed voxel is only the "tip of the iceberg." This problem is exacerbated by the fact that the smallest voxels that can be created cannot be viewed during the fabrication process, but rather must be imaged later by electron microscopy. To obtain an accurate representation of an individual voxel, an ascending scan must be performed. In this technique, identical voxels are made at different heights that range from submerged within the substrate to suspended above it.[98] In the intermediate range, the voxel will be only loosely connected to the substrate and will therefore topple over after washing, giving a clear perspective of its true size and shape (Figure 4).

As a result of the combination of optical and chemical nonlinearity, MAP can achieve a resolution that is considerably better than that predicted by the diffraction limit. The smallest individual voxel thus far reported with 800-nm excitation was 100 nm in diameter.[99] Suspended lines with widths as small as 30 nm have also been fabricated in SU-8, although this kind of resolution has not yet been achieved for more complex structures.[100] Voxels are generally ellipsoidal,

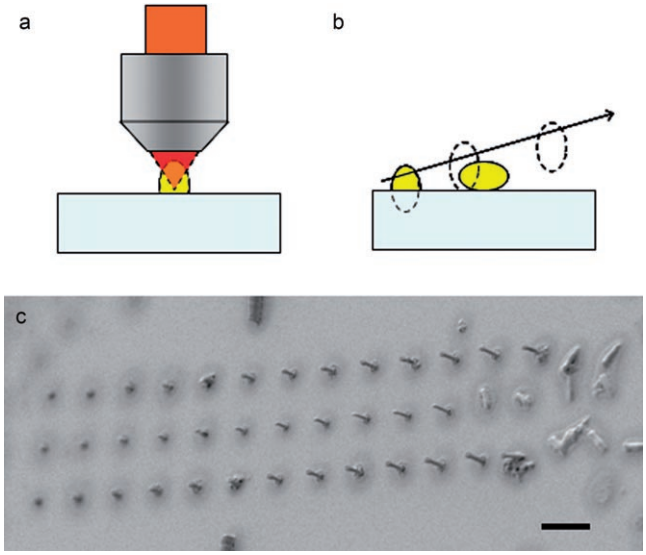

Figure 4. The ascending scan technique for measuring voxel dimensions. a) The laser is focused partly within the substrate, so that only a portion of the voxel is fabricated. b) The stage is translated to a new position and lowered slightly for the fabrication of each subsequent voxel. c) At a certain height of the focal point above the substrate, the voxels will barely adhere to the surface and will tip over during development, making their dimensions readily visible by electron microscopy. The scale bar in (c) is 10 μm.

and the two minor axes perpendicular to the optical axis are about 3–5 times smaller than the major axis.[98] This shape is determined in part by the point-spread function (PSF) of the light intensity near the focus.

The probability for TPA is proportional to I^2, which effectively narrows the PSF of the beam near the focal point so that it is smaller than the diffraction limit at the excitation wavelength. However, this narrowing alone is not sufficient to explain the decrease in voxel size that is observed experimentally.[101] In fact, voxels of comparable size have also been fabricated by using single-photon absorption.[37] The real benefit of the optical nonlinearity of TPA lies in the negligible absorption away from the focal point. Photoinitiator concentrations can be employed that are approximately ten times higher than would be feasible for single-photon excitation, yet without any fear of out-of-plane polymerization.

Chemical nonlinearity is also an important factor in the creation of voxels that are smaller than the diffraction limit. Because of quenching processes, there is a threshold intensity below which the polymerization reaction cannot be sustained to create a solid structure. By careful control of the laser intensity, this threshold can be exceeded in only a small fraction of the focal volume. For example, a beam that is focused to a 400-nm diffraction-limited spot may exceed the intensity threshold in only a 100-nm-wide region in the center of the spot.

The ultimate dimensions of a voxel are governed by factors such as the photoinitiator concentration, the radical quantum yield, the viscosity of the resin, and the concentration of any inhibitors, such as dissolved oxygen. Although no rigorous theory has been put forth that covers all of these parameters, Chichkov and co-workers have developed a simple model that fits many of the available experimental data.[85] Their model assumes a laser beam with a Gaussian profile and a square temporal pulse shape. It is further assumed that a threshold concentration of radicals is required to form a sustainable, solid polymer voxel. The model predicts the rate of change of radical concentration as a function of position and time, and defines a voxel as the volume within which the radical concentration is above the survival threshold.

The above model does not take into account diffusion, which should play an important role in determining the voxel shape in liquid resins. The incorporation of viscosity in a realistic model is challenging, as this parameter changes over the course of the polymerization reaction. Linear-exposure theory predicts that if all other parameters are kept constant, the voxel dimensions should depend only on the product of the exposure time and the square of the laser power. DeVoe et al.[102] and Sun et al.,[103] in studying the scaling laws for voxel dimensions, have demonstrated deviations from this theory. Sun et al. proposed that voxels grow by two different mechanisms.[103] One mechanism, which they named "focal-spot duplication", depends on the PSF of the focused laser beam. The other mechanism, which they named "voxel growth", depends upon the diffusion of radicals and monomers. On short time scales, it was proposed that focal-spot duplication is responsible for the aspect ratio of the voxels. On longer time scales, the growth of the aspect ratio saturates.

Continued exposure is believed to result in slower growth, driven by diffusion, which is analogous to dark growth in cationic polymerization.[103] DeVoe et al. made similar observations for an acrylic resin.[102] In contrast, for SU-8 they observed that the aspect ratio is constant for short exposures, increases rapidly above a certain exposure dose, and then levels out for higher exposures.[104] The fact that similar behavior is observed in a solid resin indicates that a more complex model is needed to understand the dependence of voxel shape on exposure. DeVoe et al. also suggest that in media such as acrylates, in which polymerization occurs immediately (rather than in a postexposure step, as is the case for SU-8), waveguiding by voxels may be an important mechanism for voxel growth.[102]

In the case of radical polymerization, quenching is another phenomenon that must be incorporated into a realistic model. Although the inclusion of a radical inhibitor in a resin increases the fabrication threshold, it has also been shown to reduce the minimum voxel dimension.[99] The exact mechanism of this action is not well understood.

3.2.2. Mechanical Properties

Because MAP fabrication occurs in a voxel-by-voxel fashion, there is some question as to whether the mechanical properties of polymers created with this technique are comparable to those of the same materials when polymerized in a more conventional manner. The challenge in making such a comparison is finding a reliable technique for measuring the mechanical properties of microscopic structures.

To give a qualitative sense of the mechanical strength of structures created with MAP, in Figure 5 we show a tower that is 20 μm wide and 1.6 mm tall. Micrometer-sized iron filings were glued to the top of the tower so that it bent in proximity to a strong magnet. Despite the small area of adhesion of the tower to the substrate and the large forces to which it was subjected repeatedly, the tower always returned to its upright equilibrium position when the magnet was withdrawn.

The first technique to be applied to make more-quantitative measurements of the mechanical properties of a structure created with MAP was optical tweezing. Optical tweezers take advantage of photon momentum to apply forces in the piconewton range to microscopic objects.[105] Sun, Takada, and Kawata used this technique to displace and release a microcoil, and thereby measured its spring constant.[106] The four-turn coil with a diameter of 2 μm was anchored on one end to a polymer block. The other end of the coil was attached a polymer bead that was trapped with the optical tweezers. Upon release, the coil acted as an overdamped oscillator with a spring constant of 10 $nN\,m^{-1}$. This value is three to five orders of magnitude smaller than would be predicted on the basis of the macroscopic Young's modulus of SCR500 (0.46 GPa). The authors attributed this discrepancy to a difference in Young's modulus between polymers cured with MAP and those cured with ultraviolet light. As the dwell time per voxel in creating the microcoil was approximately 1 ms, they theorized that the MAP samples were cross-linked to a lesser degree than the UV-cured samples. In addition, these experiments were performed in ethanol, which is a good solvent for acrylates and so presumably swelled the polymer in the microcoil. The difference in stiffness between dry and wet sponges underscores the degree to which such swelling can affect mechanical properties.

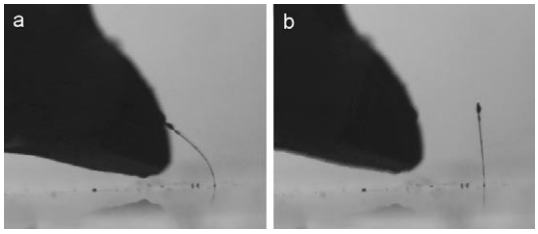

Figure 5. A 1.6 mm × 20 μm × 20 μm tower fabricated with MAP. Micrometer-sized iron filings were attached to the top of the tower. When a strong magnet is brought into close proximity (a), the tower bends. When the magnet is withdrawn (b), the tower snaps back to its original position.

The second technique to be applied to measuring the mechanical properties of objects created by MAP was atomic force microscopy (AFM). Polymer cantilevers that were fabricated with MAP were deflected with calibrated AFM cantilevers. Force versus displacement curves were obtained, allowing the spring constant of the polymer cantilever to be measured in air.[107] The Young's modulus of a cantilever can be calculated from its physical dimensions and its force constant.[108] Measurements were made on a series of cantilevers of varying dimensions, and a Young's modulus of 0.44 GPa was obtained. This modulus is comparable to that measured for a bulk sample of the same polymer that was UV cured (2 GPa).[107]

The fact that the Young's modulus of the cantilevers is smaller than that of the UV-cured polymer probably indicates that the MAP-fabricated polymers are not fully cross-linked. It will be interesting to study the effects that parameters such as exposure time, postexposure UV curing, and solvent have on the mechanical properties of structures fabricated with MAP.

3.2.3. Optical Properties

Structures fabricated by MAP have many potential applications in optics. Achieving the necessary high optical quality requires that the polymer volume be spatially homogeneous and that any optical surfaces have a roughness that is small relative to the wavelength of the light to be employed.

Attaining polymer homogeneity, and thereby optical transparency, does not present significant difficulties so long as the scanning conditions are similar throughout a structure. Figure 6a shows an electron micrograph of a complex tunnel created with MAP. Despite the significant surface roughness of this tunnel, as demonstrated by the optical micrographs in Figure 6b–d, the transparency of the tunnel is sufficient that a glass microbead can be optically trapped and transported through the structure.

Because the minimum feature size attainable in MAP is so small, it is possible with some effort to create optically smooth surfaces. The creation of flat surfaces requires smooth

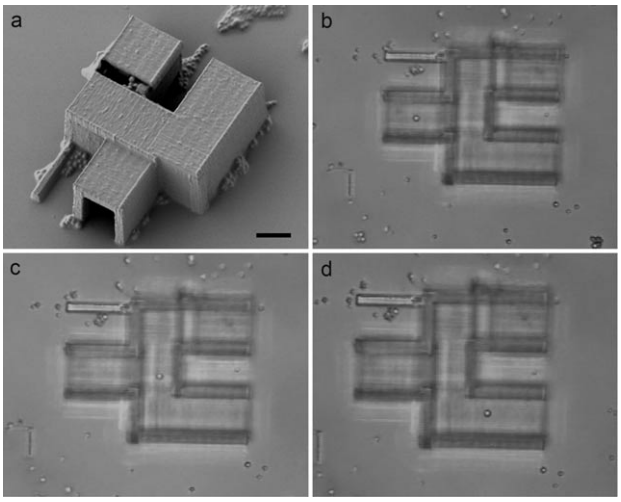

Figure 6. a) Electron micrograph of a complex tunnel created with MAP. b–d) images of a glass bead in water being optically trapped and transported through the tunnel. The scale bar in (a) is 10 μm.

scanning of the laser or sample and high laser stability, both in terms of intensity and direction. The voxel size and degree of overlap are also critical parameters in creating smooth surfaces. Takada, Sun, and Kawata demonstrated that surfaces with a mean roughness of around 8 nm can be fabricated if the distance between voxels is about 20% of the voxel size.[99] It is also believed that resins with higher viscosity tend to yield smoother structures. To illustrate the smoothness that can be achieved, Figure 7 shows a representative image of a short section of an optical waveguide.

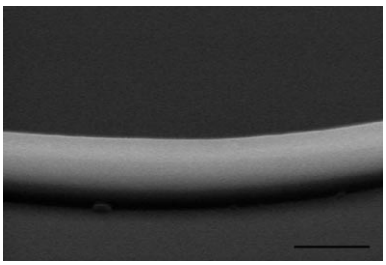

Figure 7. Section of a curved optical waveguide created with MAP, demonstrating the degree of smoothness achievable for optical applications. The scale bar is 5 μm.

4. Multiphoton Fabrication with Other Materials

Although an impressive range of structures can be created with MPA, most 3D microdevices will require the incorporation of materials other than polymers. Virtually any photochemical or photophysical process has the potential to be localized in three dimensions by using MPA. The fact that there are still relatively few demonstrations of 3D patterning of materials other than polymers by MPA is a testament to the practical difficulties that are often encountered in such processes. In this section we review the patterning of other materials either directly by MPA or onto structures that were created with MAP.

4.1. Metals

A crucial element of many applications of 3D microfabrication is the ability to interface devices with electrical circuits. Thus, it is essential to be able to incorporate metallic components into 3D microstructures. There are two basic approaches for using MPA to create 3D structures that include metals. The first approach is to use MPA to deposit metal directly and the second is to use selective chemistry to deposit metals on desired regions of 3D structures created by using MAP.

4.1.1. Direct Multiphoton Deposition of Metals

Numerous reports describe chemistry that can be used to deposit metal by either photoreduction of metal ions or photodecomposition of neutral metal-containing molecules. The most famous example of this type of chemistry is the silver halide photoreduction used in photographic processes, but there are many other metals that can be deposited with light, all of which are also candidates for patterning with MPA. A natural division for such direct deposition techniques is whether the source of metal atoms is in free solution or is held in some sort of matrix.

4.1.1.1. Deposition of Metals from Solution

Figure 8 shows two examples of 2D metal patterns that have been deposited from liquids. Following the single-photon precedents, iron metal has been deposited directly from neat iron pentacarbonyl[109,110] and gold has been deposited from a solution containing dimethylgoldhexafluoroacetylacetonate.[111] We have also reported the deposition of silver nanoparticles from a solution of silver perchlorate by using a photoreducing agent.[112] Similarly, Kawata and coworkers have demonstrated the fabrication of 2D and 3D patterns of silver and 2D patterns of gold from aqueous solutions of $AgNO_3$ and $HAuCl_4$, respectively.[113,114] In all instances the patterns are granular, but in some cases they still show good electrical conductivity.

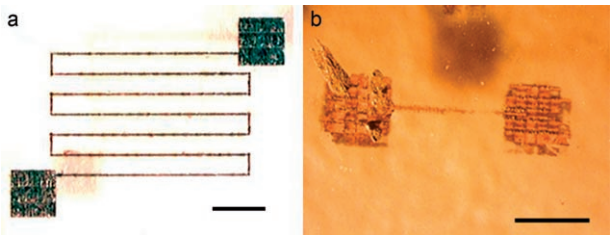

Figure 8. Two examples of the deposition of metals from liquids by TPA. a) Iron pattern deposited from neat $[Fe(CO)_5]$; the scale bar is 1 mm. b) Gold pattern deposited from dimethylgoldhexafluoroacetylacetonate in ethanol; the scale bar is 150 μm.

A number of significant problems limit the applicability of the fabrication of metallic structures from solution. The first difficulty is the above-mentioned granularity, which arises primarily because diffusion cannot replenish metal-generating species as fast as they are reduced. Thus, the concentration in the focal volume is depleted rapidly, which can terminate fabrication until the focal spot is moved to a fresh region of the solution. The second problem is that the solutions tend to boil owing to absorption of the incident laser by the deposited metal, which leads to further roughening of features and even to delamination of deposited structures. Third, metal deposited by photoreduction or photodecomposition in solution can have numerous impurities. Finally, because of the roughness of the structures and the poor mechanical properties of many easily deposited metals, freestanding structures are often not stable. For these reasons it is quite challenging to use solution-phase deposition to create high-quality 2D metallic structures, much less 3D structures.

4.1.1.2. Deposition of Metals from Matrices

An alternative technique to fabrication from metal solutions is to suspend the metal atom source in a transparent matrix. The matrix serves to support fabricated structures and can also act as a reducing agent. The first demonstration of this approach, by Wu et al., used $AgNO_3$ suspended in a silicate sol–gel matrix.[115] After fabrication, the 3D pattern of silver particles was further developed by $AgClO_4$ into dark, solid lines. The conductivity of these patterns was not measured and no attempt was made to remove the glassy matrix.

Stellacci et al. used a polyvinylcarbazole matrix infused with an organic-solvent-soluble silver salt ($AgBF_4$) and alkanethiol-coated silver nanoparticles to act as seeds for metal growth.[116] The reaction was initiated by a bis-(styryl)benzene derivative, which acted as a TPA photoreducing dye sensitizer. Using this system, they demonstrated the fabrication of a log-pile-type structure of silver lines, which was significantly deformed upon removal of the matrix. The conductivity of the metallic features was roughly three orders of magnitude lower than that of bulk silver. Copper and gold structures were also formed using salts of those metals in a poly(methyl methacrylate) matrix.

Kaneko et al. demonstrated the reduction of $HAuCl_4$ to gold in a poly(vinyl alcohol) film.[117] By interfering two ultrafast pulses in a film containing $HAuCl_4$, photoreduction resulted in the periodic patterning of gold nanoparticles over a large area. The metal patterns were not continuous or conductive, but nanoparticles were clearly formed in areas of constructive interference.

We have demonstrated a different MPA-based technique for patterning 2D metallic features on surfaces.[118] Mixing $AgNO_3$ with an ethanol-based solution of polyvinylpyrrolidone (PVP) leads to the reduction of some of the silver salt to form silver nanoparticles. This suspension can be used to cast a polymer film on a substrate, and MPA can be used to deposit smooth silver features. The polymer can then be dissolved to leave only the metallic features, which adhere strongly to the substrate. The patterns formed are granular and are not electrically conductive, but they are effective for optical applications such as the creation of efficient microscopic diffraction gratings.[118]

This work on silver patterning has been extended with the demonstration that enhancement with copper can be used to render the metallic patterns electrically conductive.[119] The conductivity could be increased to within a factor of four of that of the bulk metal. Although it was not possible to cast thick enough films of PVP to create 3D silver patterns, we have demonstrated the use of this technique to create conductive metal patterns on 3D microstructures produced with MAP.[119]

4.1.2. Chemical Deposition of Metals on 3D Microstructures

The third alternative to patterning metal in three dimensions is to deposit it chemically on an existing 3D structure. A common way to coat polymers with metal is to use an adhesion promoting agent such as $SnCl_2$. Formanek et al. demonstrated that silver can be bound to a styrene-modified SCR500 resin that is treated with $SnCl_2$ after fabrication.[120,121] By making the substrate surface hydrophobic, silver can be reduced selectively onto polymeric microstructures from an aqueous solution. The conductivity of the coating is only about a factor of five lower than that of bulk silver.

Kuebler and co-workers used the strong nucleophile $NH_2(CH_3)_2NHLi$ to modify the surfaces of acrylate, methacrylate, and epoxy polymers by amide-bond formation to give surface-bound primary amines.[122] These amines can be used to form gold seeds by reduction, and the gold can then catalyze electroless silver reduction. As granular structures are formed by the electroless deposition, the silver coating has a conductivity that is about 1.5% of that of bulk silver.

More-general approaches to selective surface modification of polymers have also been employed for metallization. We have shown that acrylates and methacrylates have different enough reactivities to enable the selective functionalization of the former polymer.[123] Polymer microstructures with some acrylic features and some methacrylic features were fabricated by MAP. The structures were treated with ethylene diamine, which reacts selectively with non-cross-linked acrylates by Michael addition to leave the methacrylates unfunctionalized (Figure 9). The amine groups on the acrylates can then be used either to reduce metal directly, as was

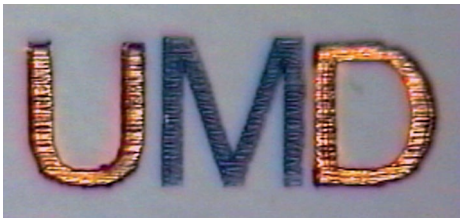

Figure 9. Selective metallization of microstructures created with MAP. The "U" and the "D" were created from an acrylic polymer and the "M" from a methacrylic polymer. Copper was deposited selectively on the acrylic structures.

demonstrated with $HAuCl_4$, or to complex a catalytic metal such as palladium, which can be used to deposit a variety of species. Palladium was used to catalyze electroless copper enhancement, forming highly conductive metallic regions on microstructures. A functional microinductor was created in this manner.[123]

Our selective functionalization scheme is quite general. Amine groups can be used to facilitate the deposition or localized synthesis of many other materials, including metal oxides and biomolecules. Furthermore, there are numerous other choices of reagents that can functionalize either methacrylates or acrylates with high selectivity.

4.2. Biomolecules

Biomolecular applications are likely to be a rapid growth area in multiphoton fabrication in the near future. There is great interest, for example, in being able to create 3D biomolecular scaffolds with spatially varying properties, an application for which multiphoton techniques are well suited. Such structures are of interest for studying the growth and interactions of cells as well as for applications in tissue engineering.

Campagnola and co-workers demonstrated the cross-linking of proteins such as bovine serum albumin (BSA), fibrinogen, and alkaline phosphatase (AP) by two- and three-photon absorption with Rose Bengal as a photosensitizer.[78,79] AP has been shown to retain enzymatic activity after cross-linking, and the degree of cross-linking, as measured by fluorescence recovery, is controllable by exposure dosage.[124,125] This technique has the potential to allow the creation of tailorable delivery devices on the micrometer scale.

Another biopolymer, collagen, has been cross-linked by using a benzophenone dimer as photosensitizer.[126] This dimer was developed as an alternative to Rose Bengal, which because of its acidity cannot be used with some proteins (such as type I and type II collagen). Two-dimensional collagen scaffolds were fabricated and used to influence dermal fibroblast growth. Campognola and co-workers also showed that the degree of cross-linking in these collagen structures could be measured by the rate of enzymatic degradation. The degradation rates are consistent with that of native collagen and can be tuned by changing the fabrication conditions.[126]

Campagnola and co-workers also demonstrated that MPA can be used to polymerize cytoplasmic proteins inside a living cell.[127] This technique could be applied as a means of physically separating intracellular components for experiments in cell biology.

Shear and co-workers have also demonstrated biological applications of MPA-based fabrication. To avoid the cytotoxicity associated with Rose Bengal, flavin adenine dinucleotide was developed as an alternative photosensitizer for cross-linking proteins.[128] This photosensitizer has been demonstrated with a number of proteins, including BSA, cytochrome *c*, glutamate dehydrogenase, and (neutr)avidin.[128] Avidin structures cross-linked with MPA retain the ability to bind biotin, which implies that cross-linking does not lead to denaturation. BSA structures were used to steer interactions during neurite growth. Voxels made of BSA have also been optically trapped and translocated through the plasma membrane of a live cell.[129] Particles of avidin were shown to retain the ability to bind biotin after trapping.

An important facet of the cross-linking of proteins is that it can be accomplished with a micro-YAG laser.[130] Shear and co-workers demonstrated the cross-linking of BSA with pulses of 532-nm light. The ability to create 3D biomolecular structures with a compact, inexpensive, turnkey laser system will facilitate the spread of this technology in biological applications.

Shear and co-workers also demonstrated a technique for metallization of cross-linked protein structures.[131] Au nanoparticles coated with biotinylated BSA bind to cytosine C microstructures through electrostatic interactions, resulting in gold-coated structures. The structures can be further developed with metal, rendering them electrically conductive. This approach may offer a means to incorporate electrical monitoring and stimulation in microbiological systems.

4.3. Other Materials

Although examples are limited so far, it is also possible to use MPA to deposit inorganic materials. Photocurable "spin-on" glasses have been reported,[132] and it is possible to create 2D patterns of these materials by using MPA. Chalcogenide glass has also been patterned with MPA.[133] As_2S_3 has an index of refraction close to 2.5 and is transparent in the near-infrared region. This transparency allows the starting material, As_4S_6 cage molecules, to be patterned by using a Ti:sapphire laser. Upon multiphoton excitation, these molecules photopolymerize into As_2S_3 glass. The unpolymerized molecules can then be etched away chemically. This reaction does not change the density of the material. The high index of refraction makes this material particularly attractive for the creation of photonic band-gap structures, but it also complicates fabrication by causing defocusing of the laser beam.

5. Applications

Although the development of MPA-based fabrication techniques is still at an early stage, quite a few applications have already been demonstrated. The majority of the applications reported so far have been in the field of optics, although interest in applications in biology, micromanipulation, and electronics is also growing.

5.1. Optics

Because it can create 3D, optically flat structures, MAP is an ideal technique for creating both planar and nonplanar components of waveguide structures. Klein et al. fabricated suspended waveguide structures between and among optical fibers,[134] including linear couplers, Y-splitters, and Mach–

Zehnder interferometers. Individual microlenses and Fresnel lenses have also been fabricated.[135]

Sherwood et al. applied MAP to fiber optics: They polished the side of a fiber to remove the cladding and then fabricated a polymeric microring resonator directly on the surface of the core.[136] The guided light inside the core couples to the microring with sharp resonances seen as dips in the transmission spectrum. The reported microring was 5 μm thick, had inner and outer diameters of 40 and 50 μm, respectively, and was robust enough to be transferred from a separate substrate to the polished fiber. The position of the microring midway along the fiber eliminates the need for external coupling to the resonator and enables multiple microrings to be placed on the same fiber. This novel design has advantages for fiber-based sensors and telecommunications devices.

Kawata and co-workers demonstrated the doping of fluorescent dyes into polymeric structures created with MAP,[137] and Yokoyama et al.,[138] used these types of materials as a gain medium in a distributed feedback laser with a footprint of $100 \times 200\ \mu m^2$.

The optical application of MAP that has received the greatest attention is the fabrication of photonic crystals (Figure 10).[69,85,139–146] The creation of these devices requires fabrication of 3D structures with subwavelength features. The ability of MAP to create 3D patterns with completely controllable geometries makes it an attractive approach to the fabrication of photonic crystals. Furthermore, MAP can be used to place defects, cavities, or waveguides in arbitrary locations within photonic crystals, which represents a significant advantage over other techniques that can only create periodic structures, such as colloidal self-assembly[23] or holographic pattering.[29]

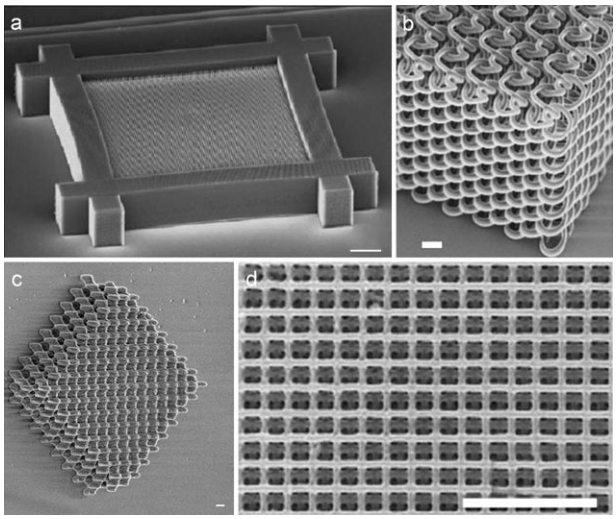

Figure 10. Examples of photonic crystals created by using MAP. a) SU-8, log-stack photonic crystal with a band gap in the near-infrared region (scale bar 10 μm; reproduced from reference [142]). b) Photonic crystal with a spiral architecture created with SU-8 (scale bar 2 μm; reproduced from reference [149]). c) Titanium-doped photonic crystal (scale bar 1 μm; image courtesy of Juan-Ming Duan). d) Silicon photonic crystal created by double inversion (scale bar 5 μm; reproduced from reference [154]).

The production of photonic crystals with MAP was first reported in 1999 by Misawa and co-workers[69] and Cumpston et al.;[54] both groups created log-stack structures. The former group measured a photonic band gap (PBG) in their structures at a wavelength near 4.0 μm, and as expected the gap red-shifted with increasing lattice spacing.[69] Wegener and co-workers demonstrated the use of SU-8 for the fabrication of a functional photonic crystal at telecommunications wavelengths (Figure 10a).[142] This photonic crystal required large side walls for support against shrinkage. Sun et al. also demonstrated the use of selective defects (missing "logs") to create a resonant cavity within a photonic crystal.[68] Braun and co-workers used MAP to polymerize structures within a colloidal photonic crystal.[147,148] Recently, more complex crystal geometries have been demonstrated, such as a diamond unit cell,[140] a spiral unit cell (Figure 10b),[149,150] and a photonic crystal with a slanted pore structure.[150,151]

Although the structures discussed above all show PBGs, the low index contrast between the polymer and the surrounding medium limits the change in transmission in the gap to typically less than 50%. The creation of a full "stop band" will require the incorporation of higher-index materials. Refractive-index contrast is a recurring problem with MAP-fabricated photonic crystals, and much effort has been devoted to solving it. One approach is to develop polymer systems with a high refractive index. For example, Ober and co-workers have demonstrated that the cationic polymerization of a brominated epoxide or of a thiirane molecule can produce materials with refractive indices of 1.62 and 1.68, respectively.[89]

Another approach to improving refractive-index contrast is the incorporation of metal oxides, such as TiO_2. These materials can be introduced into the polymer by either prefabrication doping or postfabrication infiltration with subsequent "inversion". As an example of the first approach, Kawata and co-workers used SCR500 resin doped with titanuim(IV) ethoxide to create structures with notably improved band gaps (Figure 10c).[152] Chichkov and co-workers demonstrated the infiltration of TiO_2 into 3D structures created from SU-8.[153] To accomplish infiltration, a log-stack photonic crystal was placed in a solution of titanium(IV) isopropoxide in ethanol and allowed to react with water to form nanoporous TiO_2 inside the pores of the master photonic crystal. The original SU-8 template was then removed by calcination at 600°C to yield an inverted TiO_2 photonic crystal.

A similar, but more complex, inversion scheme was also demonstrated by Wegener and co-workers for the creation of a pure silicon photonic crystal (Figure 10d):[154] This double inversion is a multistep process involving fabrication of an SU-8 template, infiltration with SiO_2, removal of the SU-8 by calcination, infiltration of the silica matrix by disilane (Si_2H_6), and removal of SiO_2 by HF. The resulting silicon photonic crystal is a faithful replica of the SU-8 master and the high refractive index of the silicon (3.7) results in a reduction in transmission by a factor of approximately 100 in the band gap at $\lambda = 2.35\ \mu m$. This wavelength can be lowered into the window for telecommunications applications at 1.55 μm by using a smaller lattice spacing, as has already been demon-

strated in an SU-8 photonic crystal.[142] One issue that should not be overlooked is the 7.5% shrinkage of SU-8 upon development. To avoid lattice distortion, photonic crystals of SU-8 must have retaining walls for structural support.

5.2. Biology

The ability to fabricate and control structures on the microscale is fundamental in the study of biological microsystems. Recent advances in MPA patterning of biopolymers and in the use of surface modification to make synthetic polymers biocompatible have already led to some remarkable results in areas such as the in situ scaffolding of cells,[127–130] as discussed in Section 4.2. Tissue scaffolding is a major growth area in MPA fabrication.

Another biologically relevant application of devices created with MAP is the manipulation of microscopic structures. Maruo, Ikuta, and Korogi fabricated micromechanical devices such as microtweezers and microneedles that can be controlled by optical trapping.[95,155–157] With a tip diameter of only 250 nm and a positioning accuracy of 15 nm, optically actuated microtweezers offer substantially better control than do electrostatic tweezers. Moreover, rastering of the trapping beam allows a number of devices to be controlled simultaneously. Optical actuation of devices will be useful in many other complex applications, including micropumps, valves, and other components of microfluidic systems.[155]

5.3. Electronics

The ability to create conductive metal coatings on structures fabricated with MAP is a recent development, so there is only one electrical application that has been reported to date. We have used MAP to create 100-μm-long functional microinductors.[123] The resonance frequencies of such inductors are in the GHz range, which is useful for communications devices, and can be lowered into the MHz range for applications in magnetic resonance. Inductors have numerous applications in electronics as filters, transformers, and components of oscillator circuits. They can also be used to generate magnetic fields for mechanical actuation or sensing, as in magnetic resonance force microscopy.[158,159]

6. Mass Production

One drawback of MPA-based fabrication techniques is that they are inherently serial processes. Structures are created on a voxel-by-voxel basis, and scaling up production to a viable level is a daunting task. Nevertheless, substantial progress has been made toward mass production.

6.1. Multipoint Fabrication

If fabrication can be accomplished at low enough laser power, one approach to mass production is to split the output of a laser into many beams that can be used to fabricate structures at different points simultaneously. Kawata and coworkers have implemented such an approach by splitting up their laser beam with a microlens array (MLA).[120,121,160] Placing the MLA in the beam path before the objective creates hundreds of focal spots, each of which can be used for MAP fabrication. The resolution of fabrication at each focal point is similar to that of the objective. This method is well-suited for the creation of periodic structures or of arrays of identical structures. However, to deliver enough power to each focal spot, an amplified laser system must be employed. Furthermore, nonuniformities in the intensity across the MLA can cause the voxel size to vary from focal point to focal point.

It is technically feasible to create a multipoint fabrication system in which the intensity of each focal point can be controlled independently by a spatial light modulator (SLM). With such a system it would be possible to fabricate nonperiodic structures in a highly parallel fashion. It should be possible to increase throughput by three orders of magnitude or more with an efficient enough photoinitiator.

6.2. Interference Lithography

Interference lithography techniques offer another means of creating complex 3D structures. Although interference techniques can be implemented with single-photon absorption,[30,31] the use of MPA can lead to significant improvements in feature size. The most common such technique is multibeam interference lithography (MBIL).[161–163] In MBIL, three or more laser beams approach a photoresist from different directions. The polarization of each beam can be controlled independently. Together the beams create a complex, 3D interference pattern that can be used to expose the photoresist. If an amplified laser is used, large beam diameters can be employed so that sizeable sample areas can be exposed in a short period of time. MBIL necessarily creates periodic 3D structures, and so is well-suited for fabrication of photonic crystal materials. If defects are desired, they can be fabricated subsequently in the photonic crystals by conventional MAP.

Rogers and co-workers developed an alternative type of interference lithography, which they call proximity-field nanopatterning (PnP).[161,164,165] In this technique, a relief pattern is created on the surface of a piece of polydimethylsiloxane (PDMS) elastomer. The PDMS is then pressed against a thick layer of photoresist on a substrate. The relief pattern in the elastomer acts as a phase mask to create a complex (but calculable) 3D interference pattern that is used to expose the photoresist. As with MBIL, PnP was originally implemented with single-photon absorption, but its resolution can be improved substantially with MPA.[161] One advantage of PnP over MBIL is that the relief pattern can vary over the surface of the mask, which can potentially be as large as a silicon wafer. Thus, although the patterns created must be at least quasiperiodic on a local scale, they can vary considerably over a distance scale as small as 10 μm.

6.3. Molding

Another approach to mass production is the use of MAP to fabricate master structures that are then replicated in a parallel manner. This approach is analogous to conventional photolithography, which also begins with the slow, serial process of mask writing. Masks enable rapid, parallel patterning on the wafer scale.

With this idea in mind, we explored the use of a soft-lithographic technique known as microtransfer molding (μTM)[12] for the replication of structures created with MAP.[166] In μTM, PDMS is cured over master structures to create an elastomeric mold. This mold is released from the master structures, filled with a molding material, and pressed against a new substrate. The molding material is then cured and the mold is released once again. Many molds can be created from a single set of master structures, and each mold can be used to create many replicas.

Although μTM enables the rapid replication of structures created with MAP, one might suppose that there are significant topological limitations to the sort of structures that can be replicated. For example, structures with high aspect ratios would be expected to be difficult to release, and structures with overhangs should be impossible to release. However, the elasticity of PDMS makes possible the replication of a far greater range of structures than might be imagined.[166] As an example, Figure 11a shows a structure

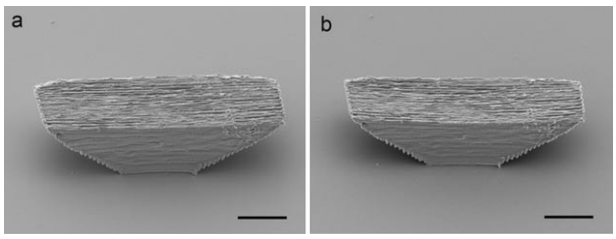

Figure 11. a) A master structure created with MAP featuring opposing overhangs with 30° open angles. b) A replica of this structure created with μTM. The scale bars are 10 μm (reproduced from reference [166]).

with two opposing overhangs with open angles of 30°. Not only can the mold be released from this structure, but, as shown in Figure 11b, the structure can also be replicated reproducibly. The PDMS is able to deform to release from these structures and then to snap back to its original shape. It is similarly possible to replicate structures with extremely high aspect ratios, such as a 300-μm tower that has a cross section of $10 \times 10\ \mu m^2$.[166]

Despite the surprising range of structures that can be replicated by μTM, it is still a "2.5-dimensional" technique, as it cannot be used to replicate structures that contain closed loops. Consider, for example, attempting to replicate a tunnel. In creating the mold, PDMS will flow into the tunnel and be cured there, locking the tunnel into the mold so that it cannot be released. We have recently developed a technique called membrane-assisted microtrasnfer molding (MA-μTM) that circumvents this "mold-lock" problem.[167] Imagine that in the middle of the tunnel master structure there is a thin membrane that stops the PDMS from making a complete loop. The PDMS, due to its elasticity, can then be released from the master structure. Flat PDMS surfaces that are in close proximity have a tendency to stick together, so by compressing the mold slightly the PDMS can adhere to itself in the membrane region. The remainder of the molding process is as usual, and the adhesion of the PDMS to itself is weak enough that the replica can be released from the mold readily. The replica differs from the original in that it now contains a closed loop. Figure 12a shows an example of a five-

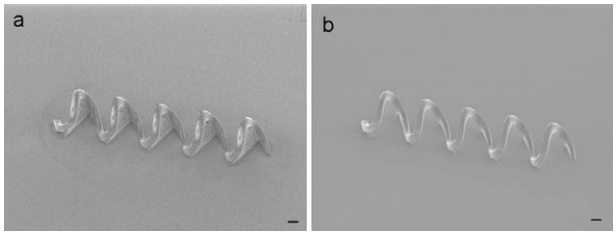

Figure 12. a) A five-turn coil master structure created with MAP. There is a membrane inside of each turn of the coil. b) Replica of the coil created by using MA-μTM. The membranes have not been replicated, leaving a structure with closed loops. The scale bars are 10 μm (reproduced from reference [167]).

turn coil with a membrane in each turn. This master structure was used to create the replica in Figure 12b in which all of the loops are open. MA-μTM makes possible the replication of a wide range of structures with closed loops, including structures with interlocking parts.[167] Furthermore, if the mold is expanded rather than compressed, it is possible to create replica structures that do contain membranes.

Not all 3D structures can be replicated with MA-μTM. There remain some topological restrictions related to mold release,[167] and any feature to be replicated must be a factor of roughly three or more thicker than the membranes. Complex structures with large numbers of small closed loops, such as photonic crystals, are not likely to be able to be replicated with MA-μTM. However, this technique does vastly expand the range of structures that can be replicated, and when combined with a suitable technique for creating wafer-scale masters MA-μTM promises to open the door to rapid mass production of structures created with MAP.

7. Outlook

The work discussed above only scratches the surface of what will one day be accomplished with MPA-based fabrication. In this section we discuss some of the major challenges in MPA-based fabrication and some of the improvements that are on the horizon.

7.1. Materials

There are many materials improvements that would be useful for specific applications of MPA-based fabrication,

such as increasing the refractive-index contrast for photonic crystals. Herein we will focus on more general materials challenges that affect a broad range of applications.

Although there are many excellent photoinitiators for MAP, there is still progress to be made. An ideal photoinitiator should be highly soluble, so that samples can be prepared quickly. It should have a high TPA cross section at 800 nm, so that a Ti:sapphire oscillator can be employed for fabrication. It should also have a high yield of reactive radicals, so that fabrication is efficient. Finding a photoinitiator that meets all of these criteria will open the door to many new applications.

Another significant materials challenge is the shrinkage that occurs in polymeric structures during the development step. For structures created with MAP to survive washing, they need to be highly cross-linked, but this cross-linking generally leads to shrinkage. Removal of unpolymerized material by solvent further augments shrinkage. It is possible in many applications to precompensate for shrinkage in the initial design, but this can be a difficult task near the substrate, where structures are tethered and cannot shrink. For some applications, such as photonic crystals, currently the only solution is to add a supporting structure to prevent shrinkage. Ultimately, overcoming the shrinkage problem will require the development of highly cross-linked materials that do not change volume appreciably during development.

The development of new patterning techniques for a broader range of materials will greatly expand the potential applications of MPA-based fabrication. The techniques discussed above have made possible the incorporation of materials such as metals into 3D structures, but means of incorporating many other materials of interest (or even multiple metals) at selected locations have yet to be demonstrated.

7.2. Resolution

The ability of MAP to create features with a resolution of 100 nm from 800-nm light is undeniably impressive. However, being able to create even smaller features is crucial to many applications, such as the creation of photonic crystals with band gaps at higher energies. Furthermore, it would be desirable to be able to create voxels that are spheres rather than prolate spheroids (see Section 3.2.1).

Part of the solution to the resolution problem may be chemical. For example, as mentioned in Section 3.2.1, the addition of radical inhibitors to a resin appears to decrease the voxel size.[99] Careful control of the polymerization chemistry may yield further decreases in voxel size, although probably only in the range of 10 to 20%. It is unclear whether chemistry can be used to improve the voxel shape as well.

Optical techniques probably offer the greatest hope for significant reductions in voxel volumes and significant improvements in voxel shapes. Optical approaches to controlling the excitation volume that may allow for modest improvements in voxel size include optimizing the focal length of the tube lens used,[168] employing annular amplitude filters,[169] and using radially polarized light.[170] Another promising technique, which has been developed in the context of fluorescence microscopy, is stimulated emission depletion (STED).[171] STED employs two laser beams, one to excite the molecules and one, which is tuned to the red of the absorption spectrum, to stimulate emission back down to the ground state. The depletion beam passes through a phase mask that causes it to be dark in the center of the focal region, so that no emission is stimulated there. As a result, it has proven possible to attain resolution of tens of nanometers in fluorescence microscopy with visible light.[172] STED also assists in creating a considerably more-spherical PSF than with standard focused laser excitation.

STED should be directly applicable to MAP. Typical radical photoinitiators become singlet diradicals upon excitation, and it is only after intersystem crossing that homolysis occurs and polymerization can be initiated.[173] The intersystem crossing time is in the range of 100 ps, so there is plenty of opportunity to stimulate emission before polymerization is initiated. In fluorescence microscopy, ideally more than 95% of molecules should be deexcited to improve resolution. In MAP it is only necessary to deexcite enough molecules to fall below the polymerization threshold; thus, stimulating emission from even 10% of the molecules may be sufficient to reduce voxel size significantly. STED may ultimately enable the creation of 20-nm voxels with 800-nm light.

7.3. Fabrication Systems

It is desirable to be able to make MPA fabrication systems more compact and less expensive. Both of these goals rely to a great extent on some of the improvements in materials discussed in Section 7.1. Beyond that, the desirable improvements in fabrication systems depend on the fabrication goals.

In a laboratory setting, it would be desirable to have a single-point fabrication system consisting of nothing more than a microscope, a laptop computer, and an inexpensive, compact, turnkey laser system. Such a fabrication system could easily fit on top of a desk or a lab bench. The use of inexpensive microlasers in place of ultrafast Ti:sapphire systems for MPA-based fabrication has already been demonstrated (Sections 3.1.2.1 and 4.2). Compact ultrafast laser systems with tens of milliwatts of power at 800 nm are also available, albeit at a somewhat greater cost. The commercial availability of highly efficient photoinitiators would make either of these laser options quite attractive.

In an industrial setting, high throughput and multipoint fabrication would be highly desirable. With efficient enough photoinitiators, such a system should be possible with a Ti:sapphire oscillator rather than an amplified laser system. The development of an SLM-based multipoint fabrication system (see Section 6.1) should then enable independent and simultaneous fabrication at 1000 or more points in a sample.

8. Conclusions

Multiphoton fabrication techniques make possible the creation of arbitrarily complex, 3D structures with sub-

micrometer feature sizes. Thanks to the efforts of research groups worldwide, the basic "toolbox" of these techniques in nearly complete. Efficient, photopolymerizable systems with a wide range of properties are now available, and it is possible to incorporate a wide variety of additional materials into microstructures. Although some additional developmental work is needed, this technology is mature enough that the focus is now shifting to applications, and we expect to see many more examples of functional devices that have been created with MPA-based techniques in the near future. As soon as the remaining obstacles to mass production are overcome, multiphoton fabrication has the potential to become an important tool in industry as well.

Abbreviations

AFM	atomic force microscopy
AP	alkaline phosphatase
BME	2-methoxy-1,2-diphenylethanone
BS	bovine serum albumin
GM	Göppert–Mayer
ITX	2-/4-isopropylthioxanthone
LIGA	Lithographie, Galvanoformung und Abformung
MA-μTM	membrane-assisted microtransfer molding
MAP	multiphoton absorption polymerization
MBIL	multibeam interference lithography
MEMS	microelectromechanical systems
MLA	microlens array
MPA	multiphoton absorption
μTAS	micro total analysis systems
μTM	microtransfer molding
NA	numerical aperture
PAG	photoacid generator
PDMS	polydimethylsiloxane
PnP	proximity-field nanopatterning
PSF	point-spread function
PVP	polyvinylpyrrolidone
SLM	spatial light modulator
STED	stimulated emission depletion
TPA	two-photon absorption
TPFM	two-photon fluorescence microscopy
YAG	Yttrium aluminum garnet

Part of the work described herein was supported by the National Science Foundation (ECS-0088438 and ECS-0210533). We are grateful for the contributions our colleagues have made to work from our laboratory that was described herein: Prof. Michael J. Naughton, Prof. Malvin C. Teich, Prof. Bahaa E. A. Selah, Prof. Michael Giersig, Dr. Michael J. R. Previte, Dr. Zeynel Bayindir, Dr. Joel Moser, Linjie Li, Juliet Znovena, Daniel Lim, Huzhen Chen, Anne-Cécile Pons, Josefina Pons, Kevin O'Malley, and Thomas Kempa.

Received: September 28, 2006
Published online: July 24, 2007

[1] J. Elders, V. Spiering, S. Walsh, *MRS Bull.* **2001**, *26*, 312.
[2] M. Esashi, T. Ono, *J. Phys. D* **2005**, *38*, R223.
[3] K. Petersen, *Sens. Actuators A* **1996**, *56*, 143.
[4] P. Grabiec, K. Domanski, P. Janus, M. Zaborowski, B. Jaroszewicz, *Bioelectrochemistry* **2005**, *66*, 23.
[5] D. R. Reyes, D. Iossifidis, P.-A. Auroux, A. Manz, *Anal. Chem.* **2002**, *74*, 2623.
[6] P. S. Dittrich, K. Tachikawa, A. Manz, *Anal. Chem.* **2006**, *78*, 3887.
[7] *The International Technology Roadmap for Semiconductors*, Semiconductor Industry Association, San Jose, **2005**.
[8] Y. Wang, T. Miyamatsu, T. Furukawa, K. Yamada, T. Tominaga, Y. Makita, H. Nakagawa, A. Nakamura, M. Shima, S. Kusumoto, T. Shimokawa, K. Hieda, *Proc. SPIE-Int. Soc. Opt. Eng.* **2006**, *6153*, 61530A.
[9] D. Ginger, S. H. Zhang, C. A. Mirkin, *Angew. Chem.* **2004**, *116*, 30; *Angew. Chem. Int. Ed.* **2004**, *43*, 30.
[10] S. Y. Chou, *MRS Bull.* **2001**, *26*, 512.
[11] M. Geissler, Y. Xia, *Adv. Mater.* **2004**, *16*, 1249.
[12] Y. Xia, G. M. Whitesides, *Angew. Chem.* **1998**, *110*, 568; *Angew. Chem. Int. Ed.* **1998**, *37*, 550.
[13] G. M. Gratson, F. Garcia-Santamaria, V. Lousse, M. J. Xu, S. H. Fan, J. A. Lewis, P. V. Braun, *Adv. Mater.* **2006**, *18*, 461.
[14] D. Therriault, R. F. Shepherd, S. R. White, J. A. Lewis, *Adv. Mater.* **2005**, *17*, 395.
[15] T. C. Wang, R. E. Cohen, M. F. Rubner, *Adv. Mater.* **2002**, *14*, 1534.
[16] J. G. Fleming, S. Y. Lin, I. El-Kady, R. Biswas, K. M. Ho, *Nature* **2002**, *417*, 52.
[17] X. M. Zhao, Y. Xia, G. M. Whitesides, *Adv. Mater.* **1996**, *8*, 837.
[18] D. W. L. Tolfree, *Rep. Prog. Phys.* **1998**, *61*, 313.
[19] J. Hruby, *MRS Bull.* **2001**, *26*, 337.
[20] P. Calvert, *Chem. Mater.* **2001**, *13*, 3299.
[21] B.-J. de Gans, P. C. Duineveld, U. S. Schubert, *Adv. Mater.* **2004**, *16*, 203.
[22] G. M. Gratson, M. J. Xu, J. A. Lewis, *Nature* **2004**, *428*, 386.
[23] Y. Xia, B. Gates, Y. Yin, Y. Lu, *Adv. Mater.* **2000**, *12*, 693.
[24] A. C. Edrington, A. M. Urbas, P. DeRege, C. X. Chen, T. M. Swager, N. Hadjichristidis, M. Xenidou, L. J. Fetters, J. D. Joannopoulos, Y. Fink, E. L. Thomas, *Adv. Mater.* **2001**, *13*, 421.
[25] U. Feldkamp, C. M. Niemeyer, *Angew. Chem.* **2006**, *118*, 1888; *Angew. Chem. Int. Ed.* **2006**, *45*, 1856.
[26] J. A. Lewis, G. M. Gratson, *Mater. Today* **2004**, *7*, 32.
[27] E. W. Becker, W. Ehrfeld, D. Muenchmeyer, Institut für Kernverfahrenstechnik, Kernforschungszentrum Karlsruhe, Karlsruhe, **1984**, p. 92.
[28] W. Ehrfeld, E. W. Becker, *KFK-Nachr.* **1987**, *19*, 167.
[29] M. Campbell, D. N. Sharp, M. T. Harrison, R. G. Denning, A. J. Turberfield, *Nature* **2000**, *404*, 53.
[30] S. Shoji, H.-B. Sun, S. Kawata, *Appl. Phys. Lett.* **2003**, *83*, 608.
[31] S. Shoji, S. Kawata, *Appl. Phys. Lett.* **2000**, *76*, 2668.
[32] S. Jeon, J. U. Park, R. Cirelli, S. Yang, C. E. Heitzman, P. V. Braun, P. J. A. Kenis, J. A. Rogers, *Proc. Natl. Acad. Sci. USA* **2004**, *101*, 12428.
[33] C. Duty, D. Jean, W. J. Lackey, *Int. Mater. Rev.* **2001**, *46*, 271.
[34] D. Lim, Y. Kamotani, B. Cho, J. Mazumder, S. Takayama, *Lab Chip* **2003**, *3*, 318.
[35] A. Bertsch, H. Lorenz, P. Renaud, *Sens. Actuators A* **1999**, *73*, 14.
[36] A. Bertsch, S. Jiguet, P. Bernhard, P. Renaud in *Rapid Prototyping Technologies* (Eds.: A. Pique, A. S. Holmes, D. B. Dimos), Materials Research Society, Warrendale, PA, **2003**, p. 3.
[37] S. Maruo, K. Ikuta, *Sens. Actuators A* **2002**, *100*, 70.
[38] K. Ikuta, S. Maruo, T. Hasegawa, T. Adachi, A. Takahashi, K. Ikeda in *Rapid Prototyping Technologies* (Eds.: A. Pique, A. S.

Holmes, D. B. Dimos), Materials Research Society, Warrendale, PA, **2003**, p. 193.
[39] A. Bertsch, S. Jiguet, P. Renaud, *J. Micromech. Microeng.* **2004**, *14*, 197.
[40] M. Goppert-Mayer, *Ann. Phys.* **1931**, *9*, 273.
[41] W. Kaiser, C. G. B. Garrett, *Phys. Rev. Lett.* **1961**, *7*, 229.
[42] W. Denk, J. H. Strickler, W. W. Webb, *Science* **1990**, *248*, 73.
[43] P. T. C. So, C. Y. Dong, B. R. Masters, K. M. Berland, *Annu. Rev. Biomed. Eng.* **2000**, *2*, 399.
[44] C. Soeller, M. B. Cannell, *Microsc. Res. Tech.* **1999**, *47*, 182.
[45] C. E. Olson, M. J. R. Previte, J. T. Fourkas, *Nat. Mater.* **2002**, *1*, 225.
[46] S. Svanberg in *Ultrafast Optics IV* (Eds.: F. Krausz, G. Korn, P. Corkum, I. Warmsley), Springer, New York, **2004**, p. 437.
[47] G. Lemercier, J.-C. Mulatier, C. Martineau, R. Anemian, C. Andraud, I. Wang, O. Stephan, N. Amari, P. Baldeck, *C. R. Chim.* **2005**, *8*, 1308.
[48] H.-B. Sun, S. Kawata, *J. Lightwave Technol.* **2003**, *21*, 624.
[49] S. Kawata, H.-B. Sun, *Appl. Surf. Sci.* **2003**, *208–209*, 153.
[50] T. Baldacchini, J. T. Fourkas in *Dekker Encyclopedia of Nanoscience and Nanotechnology* (Eds.: J. A. Schwarz, C. I. Contescu, K. Putyera), Marcel Dekker, New York, **2004**, p. 3905.
[51] D. Yang, S. J. Jhaveri, C. K. Ober, *MRS Bull.* **2005**, *30*, 976.
[52] S. Wu, J. Serbin, M. Gu, *J. Photochem. Photobiol. A* **2006**, *181*, 1.
[53] M. Albota, D. Beljonne, J.-L. Bredas, J. E. Ehrlich, J.-Y. Fu, A. A. Heikal, S. E. Hess, T. Kogej, M. D. Levin, S. R. Marder, D. McCord-Maughon, J. W. Perry, H. Rockel, M. Rumi, G. Subramaniam, W. W. Webb, X.-L. Wu, C. Xu, *Science* **1998**, *281*, 1653.
[54] B. H. Cumpston, S. P. Ananthavel, S. Barlow, D. L. Dyer, J. E. Ehrlich, L. L. Erskine, A. A. Heikal, S. M. Kuebler, I. Y. S. Lee, D. McCord-Maughon, J. Qin, H. Rockel, M. Rumi, X.-L. Wu, S. R. Marder, J. W. Perry, *Nature* **1999**, *398*, 51.
[55] J. E. Ehrlich, X. L. Wu, I. Y. S. Lee, Z. Y. Hu, H. Rockel, S. R. Marder, J. W. Perry, *Opt. Lett.* **1997**, *22*, 1843.
[56] M. Rumi, J. E. Ehrlich, A. A. Heikal, J. W. Perry, S. Barlow, Z. Hu, D. McCord-Maughon, T. C. Parker, H. Roeckel, S. Thayumanavan, S. R. Marder, D. Beljonne, J.-L. Bredas, *J. Am. Chem. Soc.* **2000**, *122*, 9500.
[57] Y. Lu, F. Hasegawa, T. Goto, S. Ohkuma, S. Fukuhara, Y. Kawazu, K. Totani, T. Yamashita, T. Watanabe, *J. Mater. Chem.* **2004**, *14*, 75.
[58] M. P. Joshi, H. E. Pudavar, J. Swiatkiewicz, P. N. Prasad, B. A. Reinhardt, *Appl. Phys. Lett.* **1999**, *74*, 170.
[59] R. Kannan, G. S. He, L. Yuan, F. Xu, P. N. Prasad, A. G. Dombroskie, B. A. Reinhardt, J. W. Baur, R. A. Vaia, L.-S. Tan, *Chem. Mater.* **2001**, *13*, 1896.
[60] B. A. Reinhardt, L. L. Brott, S. J. Clarson, A. G. Dillard, J. C. Bhatt, R. Kannan, L. Yuan, G. S. He, P. N. Prasad, *Chem. Mater.* **1998**, *10*, 1863.
[61] O.-K. Kim, K.-S. Lee, H. Y. Woo, K.-S. Kim, G. S. He, J. Swiatkiewicz, P. N. Prasad, *Chem. Mater.* **2000**, *12*, 284.
[62] G. S. He, T.-C. Lin, J. Dai, P. N. Prasad, R. Kannan, A. G. Dombroskie, R. A. Vaia, L.-S. Tan, *J. Chem. Phys.* **2004**, *120*, 5275.
[63] K. D. Belfield, K. J. Schafer, Y. Liu, J. Liu, X. Ren, E. W. Van Stryland, *J. Phys. Org. Chem.* **2000**, *13*, 837.
[64] C. Martineau, R. Anemian, C. Andraud, I. Wang, M. Bouriau, P. L. Baldeck, *Chem. Phys. Lett.* **2002**, *362*, 291.
[65] I. Wang, M. Bouriau, P. L. Baldeck, C. Martineau, C. Andraud, *Opt. Lett.* **2002**, *27*, 1348.
[66] S. Jockusch, I. V. Koptyug, P. F. McGarry, G. W. Sluggett, N. J. Turro, D. M. Watkins, *J. Am. Chem. Soc.* **1997**, *119*, 11495.
[67] K. J. Schafer, J. M. Hales, M. Balu, K. D. Belfield, E. W. Van Stryland, D. J. Hagan, *J. Photochem. Photobiol. A* **2004**, *162*, 497.
[68] H.-B. Sun, V. Mizeikis, Y. Xu, S. Juodkazis, J.-Y. Ye, S. Matsuo, H. Misawa, *Appl. Phys. Lett.* **2001**, *79*, 1.
[69] H.-B. Sun, S. Matsuo, H. Misawa, *Appl. Phys. Lett.* **1999**, *74*, 786.
[70] H.-B. Sun, T. Kawakami, Y. Xu, J.-Y. Ye, S. Matsuo, H. Misawa, M. Miwa, R. Kaneko, *Opt. Lett.* **2000**, *25*, 1110.
[71] M. Miwa, S. Juodkazis, T. Kawakami, S. Matsuo, H. Misawa, *Appl. Phys. A* **2001**, *73*, 561.
[72] K. D. Belfield, X. Ren, E. W. Van Stryland, D. J. Hagan, V. Dubikovsky, E. J. Miesak, *J. Am. Chem. Soc.* **2000**, *122*, 1217.
[73] C. Decker, K. Zahouily, D. Decker, T. Nguyen, T. Viet, *Polymer* **2001**, *42*, 7551.
[74] T. Baldacchini, H. Chen, R. A. Farrer, M. J. R. Previte, J. Moser, M. J. Naughton, J. T. Fourkas in *Commerical and Biomedical Applications of Ultrafast Lasers, Vol. 4633* (Eds.: G. S. Edwards, J. Neev, A. Ostendorf, J. C. Sutherland), Bellingham, WA, **2002**, p. 136.
[75] T. Baldacchini, R. A. Farrer, J. Moser, J. T. Fourkas, M. J. Naughton, *Synth. Met.* **2003**, *135–136*, 11.
[76] T. Baldacchini, C. N. LaFratta, R. A. Farrer, M. C. Teich, B. E. A. Saleh, M. J. Naughton, J. T. Fourkas, *J. Appl. Phys.* **2004**, *95*, 6072.
[77] C. Mendonca, Universidade de Sao Paolo, personal communication, **2006**.
[78] P. J. Campagnola, D. M. Delguidice, G. A. Epling, K. D. Hoffacker, A. R. Howell, J. D. Pitts, S. L. Goodman, *Macromolecules* **2000**, *33*, 1511.
[79] J. D. Pitts, P. J. Campagnola, G. A. Epling, S. L. Goodman, *Macromolecules* **2000**, *33*, 1514.
[80] C. Li, L. Luo, S. Wang, W. Huang, Q. Gong, Y. Yang, S. Feng, *Chem. Phys. Lett.* **2001**, *340*, 444.
[81] Y. Lu, F. Hasegawa, S. Ohkuma, T. Goto, S. Fukuhara, Y. Kawazu, K. Totani, T. Yamashita, T. Watanabe, *J. Mater. Chem.* **2004**, *14*, 1391.
[82] S. Kawata, H.-B. Sun, T. Tanaka, K. Takada, *Nature* **2001**, *412*, 697.
[83] S. M. Kuebler, M. Rumi, T. Watanabe, K. Braun, B. H. Cumpston, A. A. Heikal, L. L. Erskine, S. Thayumanavan, S. Barlow, S. R. Marder, J. W. Perry, *J. Photopolym. Sci. Technol.* **2001**, *14*, 657.
[84] T. Watanabe, M. Akiyama, K. Totani, S. M. Kuebler, F. Stellacci, W. Wenseleers, K. Braun, S. R. Marder, J. W. Perry, *Adv. Funct. Mater.* **2002**, *12*, 611.
[85] J. Serbin, A. Egbert, A. Ostendorf, B. N. Chichkov, R. Houbertz, G. Domann, J. Schulz, C. Cronauer, L. Frohlich, M. Popall, *Opt. Lett.* **2003**, *28*, 301.
[86] K.-H. Haas, K. Rose, *Rev. Adv. Mater. Sci.* **2003**, *5*, 47.
[87] C. A. Coenjarts, C. K. Ober, *Chem. Mater.* **2004**, *16*, 5556.
[88] Y. Boiko, J. M. Costa, M. Wang, S. Esener, *Opt. Express* **2001**, *8*, 571.
[89] Y. Murakami, C. A. Coenjarts, C. K. Ober, *J. Photopolym. Sci. Technol.* **2004**, *17*, 115.
[90] W. Zhou, S. M. Kuebler, K. L. Braun, T. Yu, J. K. Cammack, C. K. Ober, J. W. Perry, S. R. Marder, *Science* **2002**, *296*, 1106.
[91] W. H. Teh, U. Durig, G. Salis, R. Harbers, U. Drechsler, R. F. Mahrt, C. G. Smith, H. J. Guntherodt, *Appl. Phys. Lett.* **2004**, *84*, 4095.
[92] W. H. Teh, U. Durig, U. Drechsler, C. G. Smith, H. J. Guentherodt, *J. Appl. Phys.* **2005**, *97*, 054907.
[93] X. Yin, N. Fang, X. Zhang, I. B. Martini, B. J. Schwartz, *Appl. Phys. Lett.* **2002**, *81*, 3663.
[94] K. K. Seet, S. Juodkazis, V. Jarutis, H. Misawa, *Appl. Phys. Lett.* **2006**, *89*, 024106.
[95] S. Maruo, K. Ikuta, H. Korogi, *J. Microelectromech. Syst.* **2003**, *12*, 533.

[96] S. M. Kuebler, K. L. Braun, W. Zhou, J. K. Cammack, T. Yu, C. K. Ober, S. R. Marder, J. W. Perry, *J. Photochem. Photobiol. A* **2003**, *158*, 163.
[97] T. Yu, C. K. Ober, S. M. Kuebler, W. Zhou, S. R. Marder, J. W. Perry, *Adv. Mater.* **2003**, *15*, 517.
[98] H.-B. Sun, T. Tanaka, S. Kawata, *Appl. Phys. Lett.* **2002**, *80*, 3673.
[99] K. Takada, H.-B. Sun, S. Kawata, *Appl. Phys. Lett.* **2005**, *86*, 071122.
[100] S. Juodkazis, V. Mizeikis, K. K. Seet, M. Miwa, H. Misawa, *Nanotechnology* **2005**, *16*, 846.
[101] T. Tanaka, H.-B. Sun, S. Kawata, *Appl. Phys. Lett.* **2002**, *80*, 312.
[102] R. J. DeVoe, H. Kalweit, C. A. Leatherdale, T. R. Williams in *Multiphoton Absorption and Nonlinear Transmission Processes: Materials, Theory, and Applications* (Eds.: K. D. Belfield, S. J. Caracci, F. Kajzar, C. M. Lawson, A. T. Yeates), SPIE, Bellingham, WA, **2003**, p. 310.
[103] H.-B. Sun, K. Takada, M.-S. Kim, K.-S. Lee, S. Kawata, *Appl. Phys. Lett.* **2003**, *83*, 1104.
[104] C. A. Leatherdale, R. J. DeVoe in *Nonlinear Optical Transmission and Multiphoton Processes in Organics* (Eds.: A. T. Yeates, K. D. Belfield, F. Kajzar, C. M. Lawson), SPIE, Bellingham, WA, **2003**, p. 112.
[105] A. Ashkin, *Proc. Natl. Acad. Sci. USA* **1997**, *94*, 4853.
[106] H.-B. Sun, K. Takada, S. Kawata, *Appl. Phys. Lett.* **2001**, *79*, 3173.
[107] Z. Bayindir, Y. Sun, M. J. Naughton, C. N. LaFratta, T. Baldacchini, J. T. Fourkas, J. Stewart, B. E. A. Saleh, M. C. Teich, *Appl. Phys. Lett.* **2005**, *86*, 064105.
[108] C. A. Clifford, M. P. Seah, *Nanotechnology* **2005**, *16*, 1666.
[109] J. R. Swanson, C. M. Friend, Y. J. Chabal, *J. Chem. Phys.* **1987**, *87*, 5028.
[110] X. Xu, J. I. Steinfeld, *Appl. Surf. Sci.* **1990**, *45*, 281.
[111] D. Wexler, J. I. Zink, L. W. Tutt, S. R. Lunt, *J. Phys. Chem.* **1993**, *97*, 13563.
[112] T. Kempa, R. A. Farrer, M. Giersig, J. T. Fourkas, *Plasmonics* **2006**, *1*, 45.
[113] T. Tanaka, A. Ishikawa, S. Kawata, *Appl. Phys. Lett.* **2006**, *88*, 081107.
[114] A. Ishikawa, T. Tanaka, S. Kawata, *Appl. Phys. Lett.* **2006**, *89*, 113102.
[115] P.-W. Wu, W. Cheng, I. B. Martini, B. Dunn, B. J. Schwartz, E. Yablonovitch, *Adv. Mater.* **2000**, *12*, 1438.
[116] F. Stellacci, C. A. Bauer, T. Meyer-Friedrichsen, W. Wenseleers, V. Alain, S. M. Kuebler, S. J. K. Pond, Y. Zhang, S. R. Marder, J. W. Perry, *Adv. Mater.* **2002**, *14*, 194.
[117] K. Kaneko, H.-B. Sun, X.-M. Duan, S. Kawata, *Appl. Phys. Lett.* **2003**, *83*, 1426.
[118] T. Baldacchini, A.-C. Pons, J. Pons, C. N. LaFratta, J. T. Fourkas, Y. Sun, M. J. Naughton, *Opt. Express* **2005**, *13*, 1275.
[119] C. N. LaFratta, D. Lim, K. O'Malley, T. Baldacchini, J. T. Fourkas, *Chem. Mater.* **2006**, *18*, 2038.
[120] F. Formanek, N. Takeyasu, T. Tanaka, K. Chiyoda, A. Ishikawa, S. Kawata, *Opt. Express* **2006**, *14*, 800.
[121] F. Formanek, N. Takeyasu, T. Tanaka, K. Chiyoda, A. Ishikawa, S. Kawata, *Appl. Phys. Lett.* **2006**, *88*, 083110.
[122] Y.-S Chen, A. Tal, D. B. Torrance, S. M. Kuebler, *Adv. Funct. Mater.* **2006**, *16*, 1739.
[123] R. A. Farrer, C. N. LaFratta, L. Li, J. Praino, M. J. Naughton, B. E. A. Saleh, M. C. Teich, J. T. Fourkas, *J. Am. Chem. Soc.* **2006**, *128*, 1796.
[124] S. Basu, P. J. Campagnola, *Biomacromolecules* **2004**, *5*, 572.
[125] S. Basu, C. W. Wolgemuth, P. J. Campagnola, *Biomacromolecules* **2004**, *5*, 2347.
[126] S. Basu, L. P. Cunningham, G. D. Pins, K. A. Bush, R. Taboada, A. R. Howell, J. Wang, P. J. Campagnola, *Biomacromolecules* **2005**, *6*, 1465.
[127] S. Basu, V. Rodionov, M. Terasaki, P. J. Campagnola, *Opt. Lett.* **2005**, *30*, 159.
[128] B. Kaehr, R. Allen, D. J. Javier, J. Currie, J. B. Shear, *Proc. Natl. Acad. Sci. USA* **2004**, *101*, 16104.
[129] R. Allen, R. Nielson, D. D. Wise, J. B. Shear, *Anal. Chem.* **2005**, *77*, 5089.
[130] B. Kaehr, N. Ertas, R. Nielson, R. Allen, R. T. Hill, M. Plenert, J. B. Shear, *Anal. Chem.* **2006**, *78*, 3198.
[131] R. T. Hill, J. L. Lyon, R. Allen, K. J. Stevenson, J. B. Shear, *J. Am. Chem. Soc.* **2005**, *127*, 10707.
[132] B. R. Harkness, K. Takeuchi, M. Tachikawa, *Macromolecules* **1998**, *31*, 4798.
[133] S. Wong, M. Deubel, F. Perez-Willard, S. John, G. A. Ozin, M. Wegener, G. von Freymann, *Adv. Mater.* **2006**, *18*, 265.
[134] S. Klein, A. Barsella, H. Leblond, H. Bulou, A. Fort, C. Andraud, G. Lemercier, J. C. Mulatier, K. Dorkenoo, *Appl. Phys. Lett.* **2005**, *86*, 211118.
[135] R. Guo, S. Xiao, X. Zhai, J. Li, A. Xia, W. Huang, *Opt. Express.* **2006**, *14*, 810.
[136] T. Sherwood, A. C. Young, J. Takayesu, A. K. Y. Jen, L. R. Dalton, A. T. Chen, *Photonics Technol. Lett. IEEE* **2005**, *17*, 2107.
[137] H.-B. Sun, T. Tanaka, K. Takada, S. Kawata, *Appl. Phys. Lett.* **2001**, *79*, 1411.
[138] S. Yokoyama, T. Nakahama, H. Miki, S. Mashiko, *Thin Solid Films* **2003**, *438–439*, 452.
[139] R. A. Borisov, G. N. Dorojkina, N. I. Koroteev, V. M. Kozenkov, S. A. Magnitskii, D. V. Malakhov, A. V. Tarasishin, A. M. Zheltikov, *Appl. Phys. B* **1998**, *67*, 765.
[140] K. Kaneko, H.-B. Sun, X.-M. Duan, S. Kawata, *Appl. Phys. Lett.* **2003**, *83*, 2091.
[141] F. Korte, J. Serbin, J. Koch, A. Egbert, C. Fallnich, A. Ostendorf, B. N. Chichkov, *Appl. Phys. A* **2003**, *77*, 229.
[142] M. Deubel, G. von Freymann, M. Wegener, S. Pereira, K. Busch, C. M. Soukoulis, *Nat. Mater.* **2004**, *3*, 444.
[143] R. Guo, Z. Li, Z. Jiang, D. Yuan, W. Huang, A. Xia, *J. Opt. A* **2005**, *7*, 396.
[144] M. Straub, L. H. Nguyen, A. Fazlic, M. Gu, *Opt. Mater.* **2004**, *27*, 359.
[145] S. Wu, M. Straub, M. Gu, *Polym. Prepr. Am. Chem. Soc. Div. Polym. Chem.* **2005**, *46*, 10246.
[146] J. Serbin, M. Gu, *Adv. Mater.* **2006**, *18*, 221.
[147] P. V. Braun, S. A. Pruzinsky, W. Lee, *PMSE Prepr.* **2005**, *92*, 117.
[148] S. A. Pruzinsky, P. V. Braun, *Adv. Funct. Mater.* **2005**, *15*, 1995.
[149] K. K. Seet, V. Mizeikis, S. Matsuo, S. Juodkazis, H. Misawa, *Adv. Mater.* **2005**, *17*, 541.
[150] K. K. Seet, V. Mizeikis, S. Juodkazis, H. Misawa, *Appl. Phys. Lett.* **2006**, *88*, 221101.
[151] M. Deubel, M. Wegener, A. Kaso, S. John, *Appl. Phys. Lett.* **2004**, *85*, 1895.
[152] X.-M. Duan, H.-B. Sun, K. Kaneko, S. Kawata, *Thin Solid Films* **2004**, *453–454*, 518.
[153] J. Serbin, A. Ovsianikov, B. Chichkov, *Opt. Express* **2004**, *12*, 5221.
[154] N. Tétreault, G. von Freymann, M. Deubel, M. Hermatschweiler, F. Perez-Willard, S. John, M. Wegener, G. A. Ozin, *Adv. Mater.* **2006**, *18*, 457.
[155] S. Maruo, *Polym. Prepr. Am. Chem. Soc., Div. Polym. Chem.* **2006**, *94*, 101.
[156] S. Maruo, K. Ikuta, H. Korogi in *Three-Dimensional Nanoengineered Assemblies*, (Eds.: T. M. Orlando, L. Merhari, D. P. Taylor, K. Ikuta), Materials Research Society, Warrendale, PA, **2003**, p. 269.
[157] S. Maruo, K. Ikuta, H. Korogi, *Appl. Phys. Lett.* **2003**, *82*, 133.
[158] A. Suter, *Prog. Nucl. Magn. Reson. Spectrosc.* **2004**, *45*, 239.
[159] J. A. Sidles, J. L. Garbini in *Challenges and Opportunities in Magnetic Resonance Force Microscopy* (Eds.: M. Sarikaya,

H. K. Wikiramasinghe, M. Isaacson), Materials Research Society, Warrendale, PA, **1994**, p. 25.
[160] J.-I. Kato, N. Takeyasu, Y. Adachi, H.-B. Sun, S. Kawata, *Appl. Phys. Lett.* **2005**, *86*, 044102.
[161] S. Jeon, V. Malyarchuk, J. A. Rogers, G. P. Wiederrecht, *Opt. Express* **2006**, *14*, 2300.
[162] X.-M. Duan, H.-B. Sun, S. Kawata, *J. Photopolym. Sci. Technol.* **2004**, *17*, 393.
[163] H.-B. Sun, A. Nakamura, S. Shoji, X.-M. Duan, S. Kawata, *Adv. Mater.* **2003**, *15*, 2011.
[164] S. Jeon, E. Menard, J. U. Park, J. Maria, M. Meitl, J. Zaumseil, J. A Rogers, *Adv. Mater.* **2004**, *16*, 1369.
[165] S. Jeon, V. Malyarchuk, J. O. White, J. A. Rogers, *Nano Lett.* **2005**, *5*, 1351.
[166] C. N. LaFratta, T. Baldacchini, R. A. Farrer, J. T. Fourkas, M. C. Teich, B. E. A. Saleh, M. J. Naughton, *J. Phys. Chem. B* **2004**, *108*, 11256.
[167] C. N. LaFratta, L. Li, J. T. Fourkas, *Proc. Natl. Acad. Sci. USA* **2006**, *103*, 8589.
[168] C. J. R. Sheppard, M. Gu, *Appl. Opt.* **1991**, *30*, 3563.
[169] M. Martinez-Corral, C. Ibanez-Lopez, G. Saavedra, *Opt. Express* **2003**, *11*, 1740.
[170] S. Quabis, R. Dorn, M. Eberler, O. Glockl, G. Leuchs, *Opt. Commun.* **2000**, *179*, 1.
[171] T. A. Klar, E. Engel, S. W. Hell, *Phys. Rev. E* **2001**, *64*, 066613.
[172] T. A. Klar, S. Jakobs, M. Dyba, A. Egner, S. W. Hell, *Proc. Natl. Acad. Sci. USA* **2000**, *97*, 8206.
[173] C. S. Colley, D. C. Grills, N. A. Besley, S. Jockusch, P. Matousek, A. W. Parker, M. Towrie, N. J. Turro, P. M. W. Gill, M. W. George, *J. Am. Chem. Soc.* **2002**, *124*, 14952.

